

ANATOMY OF A LOCAL-SCALE DROUGHT: APPLICATION OF ASSIMILATED REMOTE SENSING PRODUCTS, CROP MODEL, AND STATISTICAL METHODS TO AN AGRICULTURAL DROUGHT STUDY

Manuscript to be submitted to *the Journal of Hydrology – Special Issue on Drought*

Ashok K. Mishra¹, Amor V.M. Ines², Narendra N. Das³, C. Prakash Khedun⁴, Vijay P. Singh⁵,
Bellie Sivakumar⁶, James W. Hansen⁷

¹ 202 B Lowry Hall, Glenn Department of Civil Engineering, Clemson University, Clemson, SC 29634, USA. Email: ashokm@clemson.edu; akm.pce@gmail.com

² International Research Institute for Climate and Society, The Earth Institute at Columbia University, 61 Route 9W, Palisades, NY 10964, USA. Email: ines@iri.columbia.edu

³Jet Propulsion Laboratory, M/S 300-323, 4800 Oak Grove Drive, Pasadena, CA 91109, USA. Email: Naraindra.N.Das@jpl.nasa.gov

⁴ Department of Biological & Agricultural Engineering, Water Management & Hydrological Science, 321E Scoates Hall, 2117, Texas A&M University, College Station, TX 77843, USA. Email: pkhedun@tamu.edu; pkhedun@gmail.com

⁵ Department of Biological & Agricultural Engineering, Zachry Department of Civil Engineering, Water Management & Hydrological Science, 321 Scoates Hall, 2117, Texas A&M University, College Station, TX 77843, USA. Email: vsingh@tamu.edu

⁶ School of Civil and Environmental Engineering, University of New South Wales, Vallentine Annexe (H22), Level 1, Room VA139, Kensington Campus, Australia. Email: s.bellie@unsw.edu.au.

⁷ International Research Institute for Climate and Society, The Earth Institute at Columbia University, 61 Route 9W, Palisades, NY 10964, USA. Email: jhansen@iri.columbia.edu

Corresponding author: Ashok K. Mishra (ashokm@clemson.edu; akm.pce@gmail.com)

1 **Abstract**

2 Drought is of global concern for society but it originates as a local problem. It has a significant
3 impact on water quantity and quality and influences food, water, and energy security. The
4 consequences of drought vary in space and time, from the local scale (e.g. county level) to
5 regional scale (e.g. state or country level) to global scale. Within the regional scale, there are
6 multiple socio-economic impacts (i.e., agriculture, drinking water supply, and stream health)
7 occurring individually or in combination at local scales, either in clusters or scattered. Even
8 though the application of aggregated drought information at the regional level has been useful in
9 drought management, the latter can be further improved by evaluating the structure and evolution
10 of a drought at the local scale. This study addresses a local-scale agricultural drought anatomy in
11 Story County in Iowa, USA. This complex problem was evaluated using assimilated AMSR-E
12 soil moisture and MODIS-LAI data into a crop model to generate surface and sub-surface
13 drought indices to explore the anatomy of an agricultural drought. Quantification of moisture
14 supply in the root zone remains a grey area in research community, this challenge can be partly
15 overcome by incorporating assimilation of soil moisture and leaf area index into crop modeling
16 framework for agricultural drought quantification, as it performs better in simulating crop yield.
17 It was noted that the persistence of subsurface droughts is in general higher than surface
18 droughts, which can potentially improve forecast accuracy. It was found that both surface and
19 subsurface droughts have an impact on crop yields, albeit with different magnitudes, however,
20 the total water available in the soil profile seemed to have a greater impact on the yield. Further,
21 agricultural drought should not be treated equal for all crops, and it should be calculated based
22 on the root zone depth rather than a fixed soil layer depth. We envisaged that the results of this
23 study will enhance our understanding of agricultural droughts in different parts of the world.

24 *Key words: Drought anatomy, Data assimilation, Crop yield, Copulas, Root zone soil moisture*

25 **1. Introduction**

26 There is a continuous rise in water demand in many parts of the world in order to satisfy the
27 needs of growing population, rising agricultural demand, and increasing energy and industrial
28 sectors (Mishra and Singh, 2010; Singh et al., 2014). These growing water demands are further
29 challenged by the impact of droughts. Drought propagates through water resources systems in
30 virtually all climatic zones, as it is driven by the stochastic nature of hydroclimatic variables.

31 Based on the Fifth Assessment Report of the Intergovernmental Panel on Climate Change (IPCC,
32 2013), the atmospheric temperature measurements show an estimated warming of 0.85 degree
33 Celsius since 1880 and each of the last three decades has been successively warmer at the Earth's
34 surface than any preceding decade. It is anticipated that future global warming and climate
35 change will have impact on average precipitation, evaporation, and runoff, that happen to be
36 controlling factors for different types of droughts. Drought is well considered to be a global
37 concern, since about half of the earth's terrestrial surfaces are susceptible (Kogan, 1997), and it
38 had the greatest detrimental impact among all natural hazards during the 20th century (Bruce,
39 1994; Obasi, 1994).

40 Meteorological records indicated that major droughts have been observed in all continents,
41 affecting large areas in Europe, Africa, Asia, Australia, South America, Central America, and
42 North America (Mishra and Singh, 2010). A number of drought studies have been carried out to
43 investigate drought characteristics using data from multiple sources at the global scale (Sheffield
44 and Wood, 2007; Dai, 2010; Vicente-Serrano et al., 2010 ; Van Lanen et al., 2013; Wada et al.,
45 2013), national and regional scales (Rajsekhar et al., 2014; Hao and Aghakouchak, 2014; Zhang
46 et al., 2014; Houborg et al., 2012; Li et al., 2012; Svoboda et al., 2012; Wang et al., 2011), and

47 river basin levels (Tallaksen et al., 2009; Mishra and Singh, 2009; Madadgar and Moradkhani,
48 2011; Van Loon et al., 2014; Zhang et al., 2012).

49 Over the past several decades, there has been a significant improvement in the development of
50 drought indices to quantify drought events, each with its own strengths and weaknesses (Mishra
51 and Singh, 2010). The commonly used indices are: Palmer Drought Severity Index (PDSI;
52 Palmer, 1965), Crop Moisture Index (CMI; Palmer, 1968), Bhalme and Mooly Drought Index
53 (BMDI; Bhalme and Mooley, 1980), Surface Water Supply Index (SWSI; Shafer and Dezman,
54 1982), Standardized Precipitation Index (SPI; McKee et al., 1993), Reclamation Drought Index
55 (RDI; Weghorst, 1996), Soil Moisture Drought Index (SMDI; Hollinger et al., 1993), Vegetation
56 Condition Index (VCI; Liu and Kogan, 1996), and Drought Monitor (Svoboda et al., 2002).
57 Comprehensive reviews of drought indices can be found in Heim (2002) and Mishra and Singh
58 (2010). However, the challenge still remains for deriving drought indices because of the
59 uncertainty due to scaling issues to capture detailed information instead of aggregated
60 information within spatial units. In a real-world scenario, it is often noticed that within the
61 regional scale, there are multiple socio-economic impacts (i.e., agriculture, drinking water
62 supply, ecosystem health, hydropower, waste disposal, and stream health) occurring at local
63 scales individually or in combination, either located in clusters or scattered. Therefore, to reduce
64 the socio-economic impacts of a drought, the anatomy of drought needs to be understood at a
65 local scale for near real-time drought management.

66 ***1.1 Importance of local-scale drought studies***

67 With the advancement in technology (e.g., remote sensing, climate forecasts), significant
68 improvement is made in drought identification, monitoring, and with reasonable accuracy in
69 forecasting (Mishra and Singh, 2010) at a regional to global scale by aggregating hydroclimatic

70 fluxes as well as land surface characteristics. However, drought management can be improved by
71 understanding and quantifying the triggering variables at a local scale. The local-scale drought
72 analysis can partly overcome large amounts of uncertainties due to scale issues, model
73 parameter, data quality, non-availability of socio-economic information, missing microscale
74 climate, and catchment information. The local-scale drought is a subset of regional- or global-
75 scale drought, that needs special attention to improve water management. For example, drought
76 varies with space and time within a river basin (Mishra and Singh, 2009); and there are specific
77 sub-basins where drought is frequent, that needs local-scale treatment to improve water
78 management within the watershed. Similarly, agricultural drought is mainly driven by stochastic
79 and heterogeneous soil moisture, that poses a challenge to generate subsurface drought (soil
80 moisture) information. However, with recent development of Soil Moisture Active and Passive
81 (SMAP) mission products, it is expected that the robustness of agricultural drought monitoring
82 and forecasting information will improve. Our focus in this study is limited to local-scale
83 agricultural drought analysis to improve agricultural water management.

84 ***Application to agricultural drought:*** Different crops are grown in different parts of the world,
85 regions, and even within the same watershed. When compared with that of other types of
86 drought, agricultural drought quantification is not as straightforward due to several reasons, for
87 example, crop water requirements are different for different crops, which make it complex to
88 quantify drought appropriately. Here, crop water requirement is defined as the amount of water
89 needed by the crop to grow optimally and to compensate for the loss through evapotranspiration.
90 Given a drought situation, different crops will behave differently, which means the drought for
91 one type of crop may not represent the same condition for other types of crop (i.e., drought for
92 crop may not be a drought condition for another crop). The agricultural drought will differ

93 between crops because of two major factors (demand and supply), that are discussed in the
94 following section:

95 (A) Crop water demand: The agricultural drought index should be represented by the crop
96 water availability during the growing season, that varies among crops and seasons. This is
97 governed by several factors (FAO; <http://www.fao.org/docrep/s2022e/s2022e07.htm>):

98 (a) Climate factors: Comparatively higher crop water needs are found in areas that are
99 hot, dry, windy, and sunny. Climate factors also influence the duration of the total
100 growing period and the various growth stages;

101 (b) Crop type: Higher leaf area (example: maize) will be able to transpire and, thus, use
102 more water than the reference grass crop;

103 (c) Growth type: Crops that are fully developed will require more water than those at
104 growth stages;

105 (d) Total growing period: This is an important variable, as it mostly depends on local
106 circumstances (e.g. local crop varieties). The growing periods largely differ, depending
107 on the type of crops, for example, sugarcane (270–365 days), maize grain (125–180
108 days), cotton (180–195 days), and sunflower (125–130 days). The total growing period
109 (T) also determines crop growth stages, that include initial stage (0.1 T), crop
110 development stage (0.7 to 0.8 T), and mild to late season stage (0.1 to 0.2 T);

111 (e) Crop water needs: This information needs to be collected at local scale, as it is driven
112 by several factors (a–d). For example, maize needs 500–800 mm of water, sunflower
113 needs 600–1000 mm of water, whereas sugarcane needs 1500–2500 mm of water; and

114 (f) Drought resistance: Some of the crops are more sensitivity to drought in comparison
115 to others, for example, crops with low sensitivity (cotton), medium to high sensitivity
116 (maize), and high sensitivity (potato and sugarcane).

117 (B) Crop water supply: The water is supplied to crops by the soil moisture available in the
118 root zone. Therefore, to quantify an agricultural drought index, the relationship between water
119 extraction and root zone needs to be understood. In general, more water is extracted from the top
120 layer in comparison to the bottom layers. For example, in the case of corn (Figure 1), the typical
121 extraction pattern follows 4-3-2-1 rule (Kranz et al., 2008). This means that the top 1/4th of the
122 root zone supplies 40% of the water, the next 1/4th of the root zone supplies 30% of the water,
123 and so on. Typically, the corn root depth can reach up to 180 cm, however, in some cases during
124 late season the conservative management assumes a 90 cm effective root zone. The root depth,
125 that supplies moisture for crop growth, differs between crops; therefore, soil moisture commonly
126 used for agricultural drought monitoring should be driven by the root zone depth instead of a
127 fixed depth. This means, identifying the number of layers will play an important role for
128 quantifying agricultural droughts.

129 Previous agricultural drought research considered uniform depth of soil moisture for all types of
130 available crops to quantify agricultural drought scenarios. However, as discussed above, the
131 moisture available in different layers and root zone depth will play an important role for the
132 quantification of agricultural drought. The other advancement that will be made in this study is to
133 explore the improvement made by a data assimilation-crop modeling framework by including
134 remotely-sensed soil moisture and leaf area index for agricultural drought research. Therefore,
135 the overall aim of this study is to evaluate the anatomy of a local-scale drought. This is done
136 through the following specific objectives: (a) identification of the best data assimilation-crop

137 modeling framework under different schemes for agricultural drought quantification; (b)
138 generation of surface and subsurface drought indices useful for local-scale drought analysis; (c)
139 characterization of the behavior of surface and subsurface droughts and extraction of useful
140 information for future agricultural water management; and (d) quantification of the impact of
141 surface and subsurface drought properties. Here, the agricultural drought was analyzed,
142 considering maize as a crop product.

143 **2. Experimental set up**

144 This experiment uses a combination of models (Figure 2a) to help us mine the possible
145 relationship that may exist between the different variables and to quantify the physical process in
146 the local scale agricultural droughts. For this study, we applied our modeling framework to
147 study the anatomy of a local-scale agricultural drought and its impact on maize yields in Story
148 County, Iowa, USA. The following section briefly describes different components used to
149 develop the modeling framework.

150 ***2.1 Crop model-data assimilation framework***

151 Assimilating remote sensing data into a crop simulation model by means of in-season filtering
152 (e.g., Kalman or particle filters) is a relatively new area of research in agricultural modeling (de
153 Wit & van Diepen, 2007; Vazifedoust et al., 2009; Ines et al., 2013). Remote sensing data of soil
154 moisture and vegetation (e.g., LAI – Leaf Area Index, NDVI – Normalized Difference
155 Vegetation Index, etc.) are now available at regular time intervals and spatial resolutions that can
156 be used effectively in a crop model to better estimate aggregate yields. Assimilation of remote
157 sensing data helps improve the water- and energy-budget simulation in the crop model.
158 However, assimilation of remote sensing data into a physiologically-based crop model is not as
159 straightforward as it seems, because when one variable is adjusted the other dependent variables
160 must be also updated. For example, when remotely sensed LAI data is assimilated into the crop

161 model, other model variables, like biomass and leaf weight, need to be adjusted as well. In the
162 case soil profile moisture, which is physically connected with the surface soil moisture, nudging
163 is also needed when remotely-sensed near-surface soil moisture data is assimilated in the crop
164 model.

165 To accommodate the above-mentioned requirements for a crop model-data assimilation, it is
166 essential to customize the crop model to work in a data assimilation framework. This includes
167 stopping the model at daily time step or when remote sensing data is available for assimilation
168 and then restarting it for the next day (the so-called the ‘stop-and-start mechanism’) without
169 going back to the time the seed was sown. This stop-and-start mechanism requires saving all the
170 relevant variables in physical files, such that the model can remember their current values when
171 invoked to run again by accessing these auxiliary files and reading the variables’ values on run-
172 time. This capability enables the assimilation of remote sensing data whenever available and also
173 allows the updating of the related model variables by the remote sensing variable subsequently.

174 We developed a variant of the Ensemble Kalman Filter (EnKF), called Ensemble Square Root
175 Filter (Whitaker and Hamill, 2002), to simplify the use of remotely-sensed data in the data
176 assimilation procedure. The square root filter allows data assimilation without perturbing the
177 observed data; this is particularly appealing when assimilating growth variables, e.g., LAI.
178 Details of the crop model-data assimilation framework are provided in Ines et al. (2013) and the
179 data flow and assimilation steps are illustrated in Figure 2b. Forty ensemble members were
180 created for the data assimilation experiments using observed variability in soils and crop cultivar
181 characteristics. Planting density and management practices (i.e., planting and fertilizer) were
182 kept fixed based on publications for maize in Central Iowa. The crop model-data assimilation
183 framework consists of EnKF and a modified DSSAT-CSM-Maize (Jones et al., 2003; Ines et al.,

184 2013).

185 Four major cases were explored in the crop model-data assimilation: open-loop (no data
186 assimilation); and three runs using remotely-sensed (RS) data – soil moisture (SM) assimilation
187 only, LAI assimilation only, and assimilating both SM and LAI data. Results of these
188 experiments allow us to assess the utility of RS data assimilation for better estimation of
189 aggregate yields, as compared to open-loop simulation alone, as well as to evaluate the utilities
190 of those RS variables in the data assimilation and in the study of local scale drought.

191 *Data used:* Remote sensing data that were used in the experiments include MODIS-LAI (1 x 1
192 km², 8-day composite resolution; <http://reverb.echo.nasa.gov/reverb/>), AMSR-E near-surface
193 soil moisture (Njoku et al., 2003; 25 x 25 km², daily resolution (only descending);
194 <http://nsidc.org/data/amsre/>); county maize yield data were derived from USDA-NASS
195 (<http://www.nass.usda.gov>); soil data were derived from SSURGO (<http://www.nrcs.usda.gov>);
196 weather and auxiliary data were taken from Iowa State University AgClimate mesonet
197 (<http://mesonet.agron.iastate.edu/agclimate/>) and their Extension and Outreach office's
198 publications for maize in Central Iowa (<http://www.extension.iastate.edu>). Simulations were
199 done for the 2003–2009 period.

200 **2.2 Drought indices**

201 The drought indices are the prime variable for assessing the effect of a drought and for defining
202 different drought parameters, which include intensity, duration, severity, and spatial extent. The
203 most commonly used timescale for drought analysis is a month, however, we have used weekly
204 timescale during crop periods to evaluate the agricultural drought. The drought indices are
205 calculated based on fitting a suitable probability density function for the time series, which is
206 then transformed to a normal distribution so that the mean SPI for the location and desired period

207 is zero (McKee et al., 1993). The drought indices are classified in two categories: (a) surface
208 drought indices, and (b) subsurface drought indices. A brief discussion of these is provided next.

209 ***Surface drought indices:*** The surface drought indices are derived by surface hydroclimatic
210 fluxes (i.e., precipitation, evapotranspiration and runoff), as shown in Figure 3. When
211 precipitation is standardized to quantify a drought, it is called Standardized Precipitation Index
212 (SPI). To develop a drought index, relatively longer data sets will be useful. Here, we have used
213 weekly timescale due to two reasons: (i) it will better quantify the dynamics of moisture supply
214 and demand for an agricultural drought scenario; and (ii) it will overcome some limitations of
215 length of data, which are often witnessed in the application of remote sensing products (Njoku et
216 al., 2003). The derivation of SPI based on weekly rainfall at different temporal resolution (1, 2,
217 3, 4 weeks) leads to the generation of corresponding SPI time series, SPI1, SPI2, SPI3 and SPI4.

218 ***Subsurface drought indices:*** The subsurface drought indices are derived by subsurface
219 hydrologic fluxes, which are mostly quantified by the soil moisture available at different layers
220 (Figure 3). The soil profiles were set up in the crop model-data assimilation using nine layers (0–
221 5, 5–15, 15–30, 30–45, 45–60, 60–90, 90–120, 120–150, and 150–180 cm) for a depth of 180 cm
222 sampled in a Monte Carlo way from two dominant soil types in the county based on SSURGO
223 data. Subsurface drought indices are relatively complex in comparison to the surface drought
224 indices due to challenges involved in determining: (a) moisture available in different layers; and
225 (b) root zone depth is different between crops – this makes it difficult to identify depths of soil
226 layers corresponding to the root zone depth for agricultural drought analysis. We have selected
227 different subsurface drought indices, that vary with soil layer depth (i.e., 1st layer, 2nd layer, ...)
228 as well as with temporal resolution (i.e., 1- to 4-week temporal scale). The selected drought
229 indices are:

230 (a) Standardized Soil Moisture Index for Layer 1 (SSMI_L1): This corresponds to the
231 amount of soil moisture available in the top layer (0 to 5 cm). The SSMI_L1 is calculated
232 for 1 to 4 weeks of temporal resolution, that are denoted by SSMI1_L1, SSMI2_L1,
233 SSMI3_L1, and SSMI4_L1.

234 (b) Standardized Soil Moisture Index for Layer 2 (SSMI_L2): This corresponds to the
235 amount of soil moisture available in the 2nd layer (5 to 15 cm). The SSMI_L2 is
236 calculated for 1 to 4 weeks of temporal resolution, that are denoted by SSMI1_L2,
237 SSMI2_L2, SSMI3_L2 and SSMI4_L2.

238 (c) Standardized Soil Moisture Index for Layer 3 (SSMI_L3): This corresponds to the
239 amount of soil moisture available in the 3rd layer (15 to 30 cm). The SSMI_L3 is
240 calculated for 1 to 4 weeks of temporal resolution, that are denoted by SSMI1_L3,
241 SSMI2_L3, SSMI3_L3 and SSMI4_L3.

242 (d) Standardized Soil Water Availability Index (SSWI): This corresponds to the amount of
243 soil water available in all the soil layers (0 to 180 cm) considered for the analysis. The
244 SSWI is calculated for 1 to 4 weeks of temporal resolution, that is denoted by SSWI1,
245 SSWI2, SWI3 and SSWI4. The soil water varies for different layers and there is also a
246 feedback mechanism that works to supply moisture from the bottom layer to the top layer
247 due to the suction properties of root system and the pressure differentials caused by
248 atmospheric demand. Therefore, using higher depth (180 cm) may provide aggregated
249 information of soil moisture, which could be used during drought scenarios.

250 ***2.3 Analysis of drought and yield relationship***

251 Drought-yield relationship is non-linear because of the complexity of water-yield relationship.
252 Crop sensitivities to water stress vary by crop development stage (Doorenbos and Kassam, 1979;
253 Steduto et al., 2012; Mishra et al., 2013). When a drought event occurs at the non-sensitive stage

254 of crop growth, the impact may not be as substantial as when the drought event happened at the
255 sensitive crop growth stage (e.g., during flowering). The severity and duration of a drought event
256 may also define the extent of impact to the crops. For this local-scale drought analysis, we focus
257 on the impact of drought severity, duration, maximum severity, maximum duration, number of
258 events, and the temporal scales of these drought indices to maize yields in Story County, Iowa.
259 The uniqueness of this study lies in the parameters used to analyze the agricultural drought.
260 Agricultural drought indices were derived from soil moisture values of the first (SSMI_L1),
261 second (SSMI_L2) and third (SSMI_L3) soil layers and the total available water (SSWI)
262 simulated by the aggregate-scale crop model, while assimilating SM + LAI. Since the NASS
263 yield data were reported based only on average values, we opted to perform the drought-yield
264 analysis using the forty ensemble yield results from SM + LAI data assimilation, considering that
265 the results for 2008, which was a very wet year, may be excluded. Using the time series of yield
266 ensembles is important, because not all the spectra of yields may show the sensitivities to
267 drought events. We decomposed the yearly yield distributions, therefore, to 5th percentile, 50th
268 percentile, and 95th percentile, wherein we hypothesized that those lying in the 5th percentile
269 category will show strong response to drought events. Correlation analysis was conducted to
270 determine the relationships among the drought indices mentioned above with yield categories at
271 different temporal scales (1, 2, 3 and 4 weeks).

272 ***2.4 Application of statistical methods***

273 In this study, statistical methods were used to analyze the information generated from the
274 experiment. A brief discussion of the statistical methods employed is provided here:

275 ***Cross correlation analysis:*** A linear relationship between two sets of variables can be obtained
276 using cross-correlation analysis at different lags. In this study, cross-correlation analysis was

277 employed to denote the influence of weekly rainfall on both surface and subsurface drought
278 indices at different temporal resolutions.

279 **Mutual information:** Mutual information (MI) measures the amount of information that can be
280 obtained about one random variable by observing another (Singh, 1997). For example, The
281 estimation of MI between two variables (X and Y) depends on three probability distributions
282 $p(x)$, $p(y)$, and $p(x,y)$. In this study, MI was calculated, based on the kernel density estimation,
283 that has several advantages over the traditional histogram based method (Mishra and Coulibaly,
284 2014). A high value of MI score would indicate a strong dependence between two variables. MI
285 can measure both linear and nonlinear dependency between variables.

286 **Copulas:** Multivariate analyses are often constrained by limitations of conventional functional
287 multivariate frequency distributions that assume that the marginals are from the same family of
288 multivariate distributions. The advantage of copula (Sklar, 1959) over classical multivariate
289 distributions is that it is not constrained by the statistical behavior of individual variables. In
290 hydrology, copula has been successfully used in flood studies (e.g. Chowdhary et al., 2011;
291 Zhang and Singh, 2007), multivariate drought frequency analysis (e.g. Khedun et al., 2012;
292 Shiau and Modarres, 2009), spatial mapping of drought variables (Rajsekhar et al., 2012), and in
293 modeling the influence of climate variables on precipitation (e.g. Khedun et al., 2013). The
294 methodology for copula selection and simulation adopted in this paper follows the one presented
295 by Genest and Favre (2007).

296 **Wavelet analysis:** There has been an extensive application of wavelet analysis to hydroclimatic
297 time series (Kumar and Foufoula-Georgiou, 1997; Torrence and Compo, 1998; Labat, 2005;
298 Ozger et al., 2009; Mishra et al., 2011). In this study, the Continuous Wavelet Transform (CWT)
299 was used to decompose a signal into wavelets and generate frequency information at different

300 temporal resolutions. Similarly, the cross wavelet transform (XWT) was used to detect the
301 interactions between weekly rainfall and drought indices over multiple timescales by exposing
302 the common power in time-frequency space.

303 ***Hurst exponent:*** The Hurst exponent (H) is used to measure the persistence of a time series, that
304 either regresses to a longer term mean value or ‘cluster’ in a particular direction (Sakalauskiene,
305 2003; Mishra et al., 2009). The value of H ranges between 0 and 1, and it can be categorized into
306 two major categories: (a) a value between 0 to 0.5 indicates a random walk, where there is no
307 correlation between two present and future elements and there is a 50% probability that future
308 values will go either up or down – any series of this type are hard to predict; and (b) the value of
309 H between 0.5 and 1 indicates persistent behavior, which means the time series is trending.

310 **3. Results and discussions**

311 ***3.1 Performance of data assimilation schemes***

312 The data used in this study is the most readily available source of maize yield estimate for
313 aggregate modeling in the study area. The NASS mean yield for maize in Story Co., Iowa for the
314 2003–2009 period was 11.1 Mgha⁻¹ (standard Deviation of 0.7 Mgha⁻¹). The performance of
315 assimilation schemes is shown in Table 1. Without data assimilation (open-loop), it is apparent
316 that the crop model, even if applied in a Monte Carlo way, cannot estimate well the aggregate
317 yields, although it captures some of the interannual yield variability. For these experiments, we
318 intended to use data from only one station to represent the climate in the county, so that we can
319 test the hypothesis that assimilation of remotely-sensed soil moisture or vegetation could correct
320 the deficiencies contributed by model forcing, in this case, the scale effect of station rainfall.
321 Assimilation of remotely-sensed LAI alone did improve the yield performance from open-loop.
322 Assimilation of remotely-sensed SM did not improve the correlation from the LAI assimilation

323 performance, but improved substantially the mean bias error in aggregate yield estimates. Ines et
324 al. (2013) noted that AMSR-E SM data assimilation during very wet years (e.g., 2008) tended to
325 completely minimize the water stress experienced by crops but had caused too much leaching of
326 nitrogen from the soil profile resulting in unrealistic reduction in yields. They attributed this crop
327 model-data assimilation behavior to the bias in AMSR-E soil moisture data, which new
328 generation soil moisture satellites may be able to address, e.g., the upcoming SMAP mission.
329 Assimilating both SM and LAI substantially improved the estimation of aggregate yields,
330 suggesting that correcting both the hydrologic and plant components of a field-scale crop model
331 applied at the aggregate scale to estimate aggregate processes is very important. If we apply a
332 composite of the data assimilation schemes (e.g., assimilating LAI or SM+LAI when they are
333 performing better), a better estimate of aggregate yield can be achieved with the crop data-
334 assimilation scheme. The mutual information between weekly rainfall and subsequent soil
335 moisture available at different layers was calculated using four schemes (open loop, SM
336 assimilation, LAI assimilation, and SM+LAI assimilation), as shown in Figure 4. It was observed
337 that SM+LAI assimilation comparatively captured more information between weekly rainfall and
338 soil moisture in different layers and it is expected that this information could be potentially used
339 for drought propagation from surface to subsurface layers. Therefore, for this local-scale drought
340 analysis, we focused on analyzing the soil water fluxes generated by assimilating SM + LAI
341 (normal mode).

342 ***3.2 Selection of drought indices***

343 The cumulative sum of precipitation during the crop growing periods of 2003–2009 is shown in
344 Figure 5. Based on visual inspection, three different patterns are noticed: (a) excess rainfall
345 during 2008; (b) deficit rainfall during 2006 and 2009; and (c) normal rainfall for 2003, 2004,

346 2005, and 2007. The precipitation pattern differs between the years and this difference becomes
347 more prominent during the growing stages of crops. This precipitation variability generates a
348 series of wet and dry spells, that will impact the moisture availability for crop growth (Mishra et
349 al., 2013). This study extends the analysis to improve drought indices associated with subsurface
350 soil moisture, which evolves with precipitation variability during the crop period.

351 The standardized drought indices were derived from precipitation and hydrologic fluxes
352 generated from the crop model-data assimilation (SM+LAI) framework consisting of the EnKF
353 and a modified DSSAT-CSM-Maize crop model. Before deriving drought indices, it is important
354 to identify suitable probability density functions (pdf) that fit the selected hydroclimatic
355 variables. The pdfs of weekly precipitation and soil moisture generated for layer 1 of the soil
356 profile are shown in Figure 6. Only a limited number of runoff events were generated at a weekly
357 time scale, i.e., 16 weeks witnessed runoff out of a total of 200 weeks used in the study.
358 Therefore, considering the limited number of runoff events as well as non-suitability of proper
359 pdfs, we have neglected the hydrologic drought in our analysis. Considering that our focus is
360 limited to the anatomy of a local-scale agricultural drought, we focused more on meteorological
361 and agricultural drought indices. Using three statistical tests (Kolmogorov-Smirnov, Anderson-
362 Darling, and Chi-square test), the gamma distribution was selected for precipitation and normal
363 distribution was selected for soil moisture to derive standardized drought indices for further
364 analysis.

365 Results revealed that drought indices did not respond equally to a drought condition, which
366 means different drought conditions are likely to be observed from surface and subsurface
367 drought indices at the same time. The drought indices based on 1-week and 3-week temporal
368 scale is plotted in Figure 7. It is observed that there are often mismatches between drought

369 severities occurring during growing periods over different years. This suggests that even when
370 there is a meteorological drought, there may not be an agricultural drought, and vice versa. This
371 characteristic may likely be due to the small temporal resolution (i.e., weeks), since at such a
372 resolution there may be a continuous feedback of soil moisture from the lower layer to the upper
373 layer because of suction properties of root zones. The drought characteristics also vary along the
374 soil layers. For example, in 2009, the drought based on SPI3 continued towards the end, whereas
375 based on SSMI3_L1, the drought conditions improved and reached a normal condition because
376 of the assimilation of RS soil moisture. Therefore, despite the fact that meteorological drought
377 dominated during 2009, a satisfactory crop yield was obtained due to the moisture supply
378 available in layer 1 of the soil profile.

379 The box plot of the drought severity considering all the drought indices at a 1-week temporal
380 scale is shown in Figure 8. The drought events were selected at the zero threshold level to
381 include near- normal to extreme drought conditions. It is observed that: (a) the mean of drought
382 severity for SPI1 and SSMI1_L1 remain nearly same, although higher range is observed for
383 SSMI1_L1; (b) the mean of drought severity increases with depth from layer 1 to layer 2, and
384 maximum mean was noticed for SSWI1; (c) the extreme meteorological drought that occurred
385 during 2009 according to station rainfall data was also reflected for different soil layers as well
386 as total soil water availability up to 180 cm; and (d) a higher range was observed for soil layer 2
387 in comparison to layer 1. These findings were also observed when the temporal scale was
388 increased from 1 week to 3 weeks.

389 ***3.3 Co-evolution of rainfall and drought indices***

390 The co-evolution between rainfall and drought indices was quantified using both cross
391 correlation and wavelet analysis. The cross-correlation analysis between weekly rainfall and

392 drought indices can provide their linear strength at different lag times, which can improve
393 agricultural water management by forecasting drought information at greater lead times. Some of
394 the findings highlighted the relationship between rainfall and drought indices; however, the
395 relationship was not evaluated for agricultural droughts considering soil moisture availability for
396 crop growth at subsurface scenarios. The cross-correlation plot between weekly rainfall and
397 drought indices of different temporal scales is shown in Figure 9. As expected, weekly rainfall
398 has comparatively higher correlation strength with its direct product SPI time series in the
399 sequence SPI1, SPI2, SPI3, and SPI4. However, the pattern changes for the soil moisture
400 droughts beneath the surface, with maximum correlation observed at a temporal scale of two
401 weeks. This suggests, using weekly rainfall, one can predict SSMI2_L1 and SSMI2_L2, and it
402 may be expected that the forecasting performance might decrease with the increase in depth. The
403 maximum correlation between weekly rainfall and drought indices were observed at different lag
404 times. For example, the lag time between weekly precipitation and SSMI3_L1 and SSMI4_L1
405 happens to be 2 and 3 weeks, respectively. The soil moisture available in different layers will be
406 used at different lag times for crop growth in case the meteorological drought creeps in at the
407 weekly timescale.

408 Wavelet analysis was carried out for weekly rainfall and drought indices at different temporal
409 scales. Based on weekly rainfall, the significant power was observed at 3 to 8 weeks during
410 2008, which happens to be a wet year (Figure 10a). Similar observations were also made when
411 weekly rainfall was translated to SPI1 and SPI2. However, additional significant power was
412 observed during 2003 (normal year) based on the SPI3 and SPI4 analysis. This suggests that the
413 significant power of meteorological drought signal could not be captured by the SPI time series,
414 based on a weekly temporal scale. However, significant power could possibly be captured at

415 lower temporal scales (e.g., months). The subsurface drought indices could capture the drought
416 periods with significant powers. For example, using SSMI1_L1, the significant powers were
417 observed for both wet and dry years, whereas using coarser temporal resolution at 4 weeks
418 (SSMI4_L1), the significant powers were observed for all conditions: normal years (2003 to
419 2005) with significant power at 8–12 weeks, wet year (2008) at two significant powers (5–10 and
420 16–20 weeks), and drought year (2009) with significant power observed at 20–30 weeks (Figure
421 10b). The temporal scale length also plays an important role in capturing significant power, that
422 was observed in subsurface drought indices. The significant powers also differed when surface
423 and subsurface drought indices were compared.

424 The cross-spectral power was also investigated between weekly rainfall and drought indices to
425 evaluate their evolution over different time periods. The cross-wavelet analysis generates cross-
426 spectral power, which was calculated against a red noise background and indicated by plotting
427 black outline at the 5% significant level (Figure 11). The cross-wavelet transform also detects
428 cross magnitude and significant periods. It was observed that all the surface and subsurface
429 drought indices evolved with weekly rainfall, however, their evolution varies with different crop
430 periods. For example, SPI evolves with weekly rainfall and significant powers scattered between
431 1 and 9 weeks for different time periods, with more prominence during 2008 (Figure 11a).
432 Similarly, the weekly rainfall influences the subsurface drought indices, however, the difference
433 is observed with respect to surface drought. For example, the weekly rainfall acts differently on
434 the transition of drought from space to the top soil layer (i.e., transition from SPI1 to
435 SSMI1_L1), the cross wavelet properties change as significant powers in the range of 1–6 weeks
436 were no longer observed during 2003–2005 for SSMI1_L1 (Figure 11b). This means that the
437 weekly rainfall has high interactivity with SPI at comparatively shorter timescales in comparison

438 to SSMI1_L1. The other additional observations of significant power at 32 weeks may not
439 provide useful information as our objective is to focus on crop periods at shorter time intervals.
440 These observations could significantly predict agricultural drought conditions by combining a
441 forecasting method with the cross wavelet information (Ozger et al., 2012).

442 ***3.4 Persistence properties of drought indices***

443 The Hurst exponent (H) of SPI, SSMI_L1, SSMI_L2, SSMI_L3 and SSWI at different temporal
444 scales were calculated and compared (Figure 12). The value of H greater than 0.5 indicates that
445 the drought index time series is persistent, which are essentially black noise processes and often
446 occurs in nature (Mishra et al., 2009). It is noted that the persistence of precipitation-based SPI
447 series at a temporal resolution of 1 week is comparatively less than that at longer temporal scales
448 (2–4 weeks). Considering a 1-week temporal scale, higher persistence in soil moisture drought in
449 layer 1 is observed to be higher than SPI1; however, with increase in temporal scale to 4 weeks,
450 both the indices have similar persistent properties. Interestingly, the persistence of soil moisture
451 drought in layers 2 and 3 and total soil water availability do not change, based on their
452 aggregated temporal scale. This means that both shorter (1 week) and longer (4 week) temporal
453 scales will have similar persistence of drought progression and recession in bottom layer drought
454 indices (SSMI_L2, SSMI_L3 and STSWI). The persistence dynamics were mostly observed for
455 the SPI time series followed by the soil moisture drought in layer 1 (SSMI_L1).

456 ***3.5 Probabilistic analysis of surface and subsurface drought indices***

457 Copulas were used to evaluate the probabilistic properties of surface and subsurface droughts. In
458 order to study the relationship between duration and severity of drought events, we first
459 examined the association between these two variables graphically through Kendall's plot (K-
460 plot) and chi-plots and then selected suitable copulas that capture the dependence structure

461 between these variables for different time periods, and for precipitation, soil moisture across the
462 soil horizon, and total soil water. Data for the 2-week temporal resolution is used for illustration.

463 ***Dependence structure between drought duration and severity***

464 Figure 13 shows the K-plots for SPI2 and SSMI2_L1. A K-plot is similar to a Q-Q plot with the
465 exception that data points falling on the diagonal line are deemed independent and points above
466 (below) the diagonal indicate positive (negative) dependence. As expected, we note a positive
467 dependence between duration and severity for precipitation, soil moisture, and total water
468 availability, i.e. as drought duration lengthens, the severity of the event also increases. A similar
469 behavior is noted also for SMI2_L2, SMI2_L3, and SSWI2 (not shown here).

470 Chi-plots allow a visual assessment of the dependence structure of the whole dataset and the
471 upper and lower tails separately. Chi-plots are based on the chi-square statistics for independence
472 in a two-way table. In the case of independence, the data point will fall within the two control
473 lines. Lower (upper) tail values are those that are smaller (larger) than the mean. The first
474 column of Figure 14 shows the chi-plots for the whole dataset, and the second and third columns
475 show the lower and upper tails, respectively. Significant positive association can be noted
476 between duration and severity. The dependence appears slightly stronger in the upper tail than in
477 the lower tail. This is particularly the case for precipitation and soil moisture in soil layer 1,
478 which implies that longer drought events have more severe impacts. The behavior of
479 precipitation and soil moisture in soil layer 1 is very similar, an indication that the topmost layer
480 responds to changes in the atmospheric conditions.

481 ***Modeling and simulation of duration and severity***

482 Copula permits modeling of the dependence between duration and severity, even though the
483 marginals do not belong to the same family of distributions; for example, the duration of drought

484 events for SPI2 follows the Frechet distribution, while severity follows a lognormal distribution.
485 Copula parameters were estimated using the maximum pseudo-likelihood method from the
486 following suite of copulas: Elliptical family (Gaussian and Student's t), Archimedean (Clayton,
487 Gumbel, Frank, Joe, BB 1, BB 6, BB 7, and BB 8). The BB copulas are from the two-parameter
488 families, which can capture different degrees of dependence between the variables in the body or
489 at the tails.

490 In order to study the relationship between duration and severity of drought events, we first
491 examine the association between these two variables graphically through Kendall's plot (K-plot)
492 and chi-plots and then select suitable copulas that capture the dependence structure between
493 these variables for different time periods, and for precipitation, soil moisture across the soil
494 horizon, and total soil water. A combination of graphical and analytical methods (Akaike
495 Information Criteria) were used for the copula selection. Data for 2-week average is used for
496 illustration. The most suitable copula that deemed to capture the dependence between drought
497 duration and severity varies both across timescales and depths (Table 2). For a temporal scale of
498 2 weeks, the dependence structure for precipitation and soil moisture in the first layer can be
499 modeled via the Joe copula, and the Gaussian and Frank copulas are deemed most appropriate
500 for layer 2 and 3, respectively. Figure 15 allows a visual comparison of observed data
501 superimposed over randomly generated values from the chosen copula for SPI2 (Fig. 15(a)) and
502 SSMI2_L2 (Fig. 15(b)).

503 Averaging over timescale (i.e. going from 1 week to 4 weeks), we note that the Joe copula is the
504 preferred copula for precipitation for 1-week and 2-week scales, while the Gumbel copula is
505 better suited to model the dependence structure for 3-week and 4-week scales. Both the Joe and
506 Gumbel copulas exhibit upper tail dependence. Note that such upper tail dependence is due to the

507 one extreme event (duration of 23 weeks and associated severity of 34.6 for SPI2 and duration of
508 20 weeks and severity of 22.5 for SSMI2_L2), that dictates the behavior of the upper tail and
509 guides the choice of copula. The presence of this one extreme event is interesting, as it suggests
510 that the occurrence of extremely severe long duration drought is not impossible, and thus events
511 with intermediate characteristics is not improbable. It is also important to note that when
512 averaging over longer time scales, the tail behavior becomes less dominant.

513 Moving from the topmost soil layer to the lower layers, we note that the choice of copula again
514 changes. The topmost layer exhibits upper tail dependence, as it responds faster to the changes in
515 atmospheric conditions; that is, lack of rainfall quickly leads to soil moisture deficit and as the
516 drought lingers, it leads to the depletion of moisture in the topmost soil layer. The subsurface
517 layers respond slower to drought events. Often, even before any depletion of soil moisture starts,
518 the upper layer drought has ended. In fact, such tail behavior, as demonstrated via the K-plots
519 and chi-plots, is present in the upper tail in the precipitation and upper soil moisture data and
520 slowly disappears with depth. This behavior is further visible in the choice of copula. The copula
521 deemed suitable for the subsurface layers are the ones that do not exhibit strong upper tail
522 dependence (e.g. Gaussian and Frank).

523 **3.6. *Impact of drought on maize yields***

524 Here we present the impact of drought severity, duration, maximum severity, maximum duration
525 and number of events only to aggregated maize yields at different temporal scales. The scatter
526 plot and correlation coefficient were used to evaluate the causal effect of drought properties on
527 aggregated maize yields. It is interesting to note that drought severity does not have a strong
528 signal to the 5th percentile yields from the 1st and 2nd soil layer soil moisture (SSMI_L1,
529 SSMI_L2), although a negative slope was observed from the drought-yield relationship at

530 different temporal scales, suggesting that the higher the severity the lower the yield that can be
531 achieved at the 5th percentile category (Figure 16). However, soil moisture drought severity in
532 the 3rd soil layer (SSMI_L3) at coarser temporal scales (i.e., 2, 3 and 4 weeks) has a significant
533 impact on the 5th percentile yields, which is consistent with the analysis of Mishra et al. (2013) in
534 regards to the timing of water stress and yield relationship. More importantly, the drought
535 severity index for the total available water (SSWI) exercised the greatest impact on the 5th
536 percentile yields at different temporal scales. This suggests that of the four agricultural drought
537 parameters studied, the total profile soil moisture is the best indicator of the level of yields at
538 least at the 5th percentile based on the severity of drought. Likewise, it is important to note that
539 the temporal scale of drought severity can also compound the analysis, as for the 3-week
540 timescale, for example, lower correlation coefficient showed lesser sensitivity compared to the 1-
541 , 2-, and 4-week scales with the 2-week timescale having the strongest effect, again highlighting
542 the non-linearity of crop response to water stress, if a drought event occurred at the non-sensitive
543 period of crop growth the impact to crop yield is less severe as to when the drought occurred at
544 the sensitive period of crop growth.

545 As expected, the drought duration index for the total profile soil moisture (SSWI) gave
546 the strongest signal to impact the 5th percentile yields (Figure 17). At the 3-week timescale, this
547 signal was dampened compared to the 1-, 2-, and 4-week scales, again suggesting the non-
548 linearity in drought-yield response. The signal strength for the 3rd soil layer soil moisture
549 (SSMI_L3) actually vanished compared to drought severity. The duration of drought posed to
550 have more direct effect on the 5th percentile yields from the 1st soil layer soil moisture
551 (SSMI_L1) at timescales of 1, 2, and 3 weeks, with the last one posing the strongest signal. This

552 suggests that long duration droughts can deplete heavily the surface soil moisture and its signal
553 could be felt by the crops as this the most active layer for crop consumptive water use.

554 The maximum severity index further confirms the effectiveness of the SSWI as the best
555 index for agricultural drought (Figure 18). The strength is exceptional with r ranging from 0.86
556 to 0.94, with the strength highest for the 1-week timescale, followed by 2 and 3 weeks. The
557 SSMI_L3 also retained the significant signal in regards to the maximum severity and 5th
558 percentile yield relationship, while SSMI_L1 and SSMI_L2 were not significant, although
559 posing negative slopes as well. As regards the maximum duration index, SSWI showed the most
560 significant signal (Figure 19). In the case of the SSMI_L3, higher correlation coefficient was
561 observed in comparison to other temporal scale. The strengths for SSMI_L1 for timescales of 2–
562 4 weeks show some significant signal strengths as well. With respect to the relationship between
563 the number of events and 5th percentile yields, we found that except for SSWI at the 3- and 4-
564 week timescales, there were no significant negative relationships observed (not shown). For the
565 50th and 95th percentile yields, there were no significant negative relationships found among the
566 drought indices examined at different temporal scales, although some negative slope was
567 determined at a higher time scale (not shown).

568 **4. Conclusions**

569 Among different types of droughts, agricultural drought seems to be the most complex, as it is
570 driven by both surface (i.e., evapotranspiration) and subsurface hydroclimatic fluxes (i.e., soil
571 moisture) at a local scale. Therefore, improving our understanding of the evolution of
572 agricultural drought is necessary to develop measures to reduce the impact of drought on food
573 security. This study utilizes the assimilated AMSR-E soil moisture and MODIS-LAI data in a

574 crop model to investigate the anatomy of a local scale drought using surface and subsurface
575 hydrologic fluxes. The following conclusions are drawn from this study:

576 a) Agricultural drought differs from one crop to another. Understanding the anatomy of an
577 agricultural drought will remain a challenge due to our limited understanding of moisture
578 demand and supply for crop growth. The moisture demand is influenced by several
579 factors, and not limited to crop type, climate pattern, growing period, and their resilience
580 to drought. Quantification of moisture supply in the root zone remains a grey area in
581 research community due to the difference in root zone depth between crops and non-
582 uniform moisture supply from different soil layers. Agricultural drought monitoring
583 should be driven by the root depth instead of a fixed depth.

584 b) Assimilation of soil moisture and leaf area index into crop modeling framework might be
585 more suitable for agricultural drought quantification, as it performs better in simulating
586 crop yield. This assimilation scheme is also able to capture better information between
587 weekly precipitation and subsurface soil moisture in different layers and scale processes.

588 c) Surface and subsurface drought indices do not respond equally to a similar drought
589 condition at shorter temporal resolutions (e.g., weeks), which suggests different drought
590 conditions are likely to be observed from surface and subsurface drought indices at the
591 same time. This information is critical in evaluating the soil moisture available in
592 different soil layers for crop growth during drought periods.

593 d) The persistence of subsurface droughts is in general higher than surface droughts. The
594 dynamics in persistence were observed in SPI and soil moisture drought at 0 to 5 cm soil
595 thickness. The soil moisture drought in layers 2 and 3 and total soil water availability do
596 not change, based on their aggregated temporal scale.

597 e) Positive association between duration and severity was observed in surface and
598 subsurface drought events at all timescales. The dependence is slightly stronger at the
599 upper tail. The dependence structure, especially the presence of one long-duration high-
600 severity event, determines the choice of copula. This extreme event is more pronounced
601 in precipitation and the top soil layer but is dampened in lower layers.

602 f) It is found that the total water available in the soil profile is the best parameter for
603 describing the agricultural drought in the study region. However, it changes with crops
604 (short vs. longer root zone), climatic zones, and type of soil to retain soil moisture in
605 different layers.

606 **Acknowledgement:** We acknowledge the supports of CCAFS, NASA/JPL SERVIR project,
607 NASA SMAP Early Adopter and NOAA Cooperative Grant #NA05OAR4311004 in developing
608 the crop model-data assimilation system. We thank two anonymous reviewers for their positive
609 and constructive comments on an earlier version of this manuscript.

610

611 **References:**

612 Bhalme, H.N., Mooley, D.A., 1980. Large-scale droughts/floods and monsoon circulation. Mon.
613 Weather Rev. 108, 1197–1211.

614 Bruce, J.P., 1994. Natural disaster reduction and global change. Bull. Am. Meteorol. Soc. 75,
615 1831–1835.

616 Chowdhary, H., Escobar, L. and Singh, V., 2011. Identification of suitable copulas for bivariate
617 frequency analysis of flood peak and flood volume data. Hydrology Research, 42(2–3):
618 193–216.

619 Dai, A. 2010. Drought under global warming: a review. Wiley Interdisc. Rev. Clim.
620 Change 2, 45–65.

621 de Wit, A. J. W. & Van Diepen, C.A. (2007). Crop model data assimilation with the Ensemble
622 Kalman filter for improving regional crop yield forecasts. Agricultural Forest
623 Meteorology, 146, 38-56.

624 Doorenbos, J. & Kassam, A.H. (1979). Yield response to water. FAO Irrigation and Drainage
625 Paper No. 33. Rome, FAO.

626 FAO; Crop water needs, Chapter 3, <http://www.fao.org/docrep/s2022e/s2022e07.htm> (Date
627 accessed 25th June 2014).

628 Genest, C. and Favre, A.-C., 2007. Everything You Always Wanted to Know about Copula
629 Modeling but Were Afraid to Ask. *Journal of Hydrologic Engineering*, 12(4): 347-368.

630 Hao, Z., and AghaKouchak, A. 2014. A Nonparametric Multivariate Multi-Index Drought
631 Monitoring Framework. *J. Hydrometeorol*, 15, 89–101.

632 Heim, R., 2002. A review of twentieth-century drought indices used in the United States. *Bull.*
633 *Am. Meteorol. Soc.* 83, 1149–1165.

634 Hollinger, S.E., Isard, S.A., Welford, M.R., 1993. A New Soil Moisture Drought Index for
635 Predicting Crop Yields. In: *Preprints, Eighth Conf. on Applied Climatology*, Anaheim,
636 CA, Amer. Meteor. Soc., pp. 187–190.

637 Houborg, R., M.Rodell, B.Li, R.Reichle, and B. F.Zaitchik (2012), Drought indicators based on
638 model-assimilated Gravity Recovery and Climate Experiment (GRACE) terrestrial water
639 storage observations, *Water Resour. Res.*, 48, W0752.

640 Ines, A.V.M., Das, N.N., Hansen, J.W. & Njoku, E.G. (2013). Assimilation of remotely sensed
641 soil moisture and vegetation with a crop simulation model for maize yield prediction.
642 *Remote Sensing of Environment*. 138: 149–164. doi: 10.1016/j.rse.2013.07.018.

643 IPCC, 2013: Summary for Policymakers. In: *Climate Change 2013: The Physical Science Basis.*
644 *Contribution of Working Group I to the Fifth Assessment Report of the*
645 *Intergovernmental Panel on Climate Change* [Stocker, T.F., D. Qin, G.-K. Plattner, M.
646 Tignor, S.K. Allen, J. Boschung, A. Nauels, Y. Xia, V. Bex and P.M. Midgley (eds.)].
647 Cambridge University Press, Cambridge, United Kingdom and New York, NY, USA.

648 Jones, J.W., Hoogenboom, G, Porter, C., Boote, K. J., Batchelor, W. D., Hunt, L. A., Wilkens, P.
649 W., Singh, U., Gijsman, A. J. & Ritchie, J.T. (2003). The DSSAT Cropping System
650 Model. *European Journal of Agronomy*, 18, 235-265.

651 Khedun, C.P., Chowdhary, H., Mishra, A.K., Giardino, J.R. and Singh, V.P., 2013. Water Deficit
652 Duration and Severity Analysis Based on Runoff Derived from the Noah Land Surface
653 Model. *Journal of Hydrologic Engineering*. 18(7), 817–833.

654 Khedun, C.P., Mishra, A.K., Singh, V.P. and Giardino, J.R., 2014. A Copula-Based Precipitation
655 Forecasting Model: Investigating the Effect of Interdecadal Modulation of ENSO's
656 Impacts on Monthly Precipitation. *Water Resources Research*, 50, 580–600,
657 doi:10.1002/2013WR013763.

658 Kogan, F.N., 1997. Global drought watch from space. *Bull. Am. Meteorol. Soc.* 78, 621–636.

659 Kranz, William L., Suat Irmak, Simon van Donk, C. Dean Yonts, and Derrel L.
660 Martin. 2008. Irrigation Management for Corn. NebGuide G1850. UNL Extension
661 Division. 4 pp.

662 Li, B., et al. (2012), Assimilation of GRACE terrestrial water storage into a land surface model:
663 Evaluation and potential value for drought monitoring in western and central Europe, *J.*
664 *Hydrol.*, 446-447, 103–115.

665 Liu, W.T., Kogan, F.N., 1996. Monitoring regional drought using the vegetation condition index.
666 *Int. J. Remote Sens.* 17, 2761–2782.

667 Madadgar, S. and Moradkhani, H. 2013. Drought Analysis under Climate Change Using
668 Copula. *J. Hydrol. Eng.*,18(7), 746–759.

669 McKee, T.B., Doesken, N.J., Kleist, J., 1993. The Relationship of Drought Frequency and
670 Duration to Time Scales, Paper Presented at 8th Conference on Applied Climatology.
671 American Meteorological Society, Anaheim, CA.

672 Mishra, A. K., and Singh, V. P. (2009). Analysis of drought severity-area-frequency curves using
673 a general circulation model and scenario uncertainty. *Journal of Geophysical Research-*
674 *Atmosphere*, 114, D06120.

675 Mishra, A. K., Özger, M., and Singh, V. P. (2009). Trend and persistence of precipitation under
676 climate change scenarios. *Hydrological processes*, 23(16), 2345-2357.

677 Mishra, A. K., and Singh, V. P. (2010). A review of drought concepts. *Journal of Hydrology*,
678 391(1-2), 202-216.

679 Mishra, A. and Coulibaly, P. (2014). Variability in Canadian Seasonal Streamflow Information
680 and Its Implication for Hydrometric Network Design. *J. Hydrol. Eng.*, 19(8), 05014003.

681 Mishra, A.K., Ines, A.V.M., Singh, V.P. & Hansen. J.W. (2013). Extraction of information
682 contents from downscaled precipitation variables for crop simulations. *Stochastic*
683 *Environmental Research and Risk Assessment*. 27: 449-457. doi: 10.1007/s00477-012-
684 0667-9.

685 Njoku, E. G., Jackson, T. L., Lakshmi, V., Chan, T. & Nghiem, S.V. (2003). Soil Moisture
686 Retrieval from AMSR-E. *IEEE Transactions of Geosciences and Remote Sensing*, 41,
687 215-229.

688 Obasi, G.O.P., 1994. WMO's role in the international decade for natural disaster reduction. *Bull.*
689 *Am. Meteorol. Soc.* 75 (9), 1655–1661.

690 Ozger, M., Mishra, A. K., and Singh, V. P. (2012). Long lead time drought forecasting using a
691 wavelet and fuzzy logic combination model: a case study in Texas. *Journal of*
692 *Hydrometeorology*,13, 284–297.

693 Palmer, W.C., 1965. Meteorologic Drought. US Department of Commerce, Weather Bureau,
694 Research Paper No. 45, p. 58.

695 Palmer, W.C., 1968. Keeping track of crop moisture conditions, nationwide: the new crop
696 moisture index. *Weatherwise* 21, 156–161.

697 Rajsekhar, D., Singh, V. P., Mishra, A. K. 2014. Hydrologic drought atlas for Texas, *Journal of*
698 *Hydrologic Engineering*, (Accepted).

699 Rajsekhar, D., Singh, V.P. and Mishra, A.K., 2012. Hydrological Drought Atlas for the State of
700 Texas for Durations from 3 Months to 36 Months and Return Periods from 5 Years to
701 100 Years Department of Biological and Agricultural Engineering, Texas A&M
702 University, College Station, Tx.

703 Shafer, B.A., Dezman, L.E., 1982. Development of a Surface Water Supply Index (SWSI) to
704 Assess the Severity of Drought Conditions in Snowpack Runoff Areas. In: Preprints,
705 Western SnowConf., Reno, NV, Colorado State University, pp. 164–175.

706 Sheffield, J. & Wood, E. F. (2007). Characteristics of global and regional drought, 1950–2000:
707 analysis of soil moisture data from off-line simulation of the terrestrial hydrologic
708 cycle. *J. Geophys. Res.* 112, D17115.

709 Shiau, J.T. and Modarres, R., 2009. Copula-based drought severity-duration-frequency analysis
710 in Iran. *Meteorological Applications*, 16(4): 481-489.

711 Singh, V. P., Khedun, C. P. and Mishra, A. K. 2014. Water, Environment, Energy, and
712 Population Growth: Implications for Water Sustainability under Climate Change. *J.*
713 *Hydrol. Eng.*, 19(4), 667–673.

714 Singh, V.P. The use of entropy in hydrology and water resources. *Hydrol. Process.* 1997, 11,
715 587–626.

716 Sklar, A., 1959. Fonctions de repartition à n dimensions et leurs marges. Publications de l'Institut
717 de Statistique de l'Université de Paris, 8: 229-231.

718 Steduto, P., Hsiao, T.C. Fereres, E. & Raes, D. (2012). Crop yield response to water. FAO
719 Irrigation and Drainage Paper No. 33. Rome, FAO.

720 Svoboda, Mark, and Coauthors, 2002: The Drought Monitor. Bull. Amer. Meteor. Soc., 83,
721 1181–1190.

722 Tallaksen, L. M., Hisdal, H., and van Lanen, H. A. J.: Space-time modelling of catchment scale
723 drought characteristics, *J. Hydrol.*, 375, 363–372, 2009.

724 Van Lanen, H. A. J., Wanders, N., Tallaksen, L. M., and Van Loon, A. F. 2013. Hydrological
725 drought across the world: impact of climate and physical catchment structure, *Hydrol.*
726 *Earth Syst. Sci.*, 17, 1715–1732, doi:10.5194/hess-17-1715-2013.

727 Van Loon, A. F., E. Tjiedeman, N. Wanders, H. A. J. Van Lanen, A. J. Teuling, and R.
728 Uijlenhoet (2014), How climate seasonality modifies drought duration and deficit, *J.*
729 *Geophys. Res. Atmos.*, 119, 4640–4656.

730 Vazifedoust, M., Van Dam, J. C., Bastiaanssen, W. G. M. & Feddes, R.A. (2009). Assimilation
731 of satellite data into agrohydrological models to improve crop yield forecasts.
732 *International Journal of Remote Sensing*, 30, 2523-2545.

733 Vicente-Serrano, Sergio M., Santiago Beguería, Juan I. López-Moreno, 2010: A Multiscalar
734 Drought Index Sensitive to Global Warming: The Standardized Precipitation
735 Evapotranspiration Index. *J. Climate*, 23, 1696–1718.

736

737 Wang, D., M. Hejazi, X. Cai, A. J. Valocchi, 2011. Climate change impact on meteorological,
738 agricultural, and hydrological drought in central Illinois, *Water Resour. Res.*, 47,
739 W09527,

740 Wada, Y., van Beek, L. P. H., Wanders, N., and Bierkens, M. F. P. 2013. Human water
741 consumption intensifies hydrological drought worldwide, *Environ. Res. Lett.*, 8, 034036,
742 doi:10.1088/1748- 9326/8/3/034036.

743 Whitaker, J. S. & Hamill, T. M. (2002). Ensemble data assimilation without perturbed
744 observations. *Monthly Weather Review*, 130, 1913-1924.

745 Zhang, L. and Singh, V.P., 2007. Trivariate Flood Frequency Analysis Using the Gumbel–
746 Hougaard Copula. *Journal of Hydrologic Engineering*, 12(4): 431-439.

747 Qiang Zhang, Peng Sun, Jianfeng Li, Vijay P. Singh, Jianyu Liu, 2014. Spatiotemporal
748 properties of droughts and related impacts on agriculture in Xinjiang, China. International
749 Journal of Climatology, DOI: 10.1002/joc.4052.

750 Qiang Zhang, Vijay P. Singh, Mingzhong Xiao, Jianfeng Li, 2012. Regionalization and spatial
751 changing properties of droughts across the Pearl River basin, China. Journal
752 of Hydrology, 472-473, 355-366.

753

754

755

756

757

758

759

760

761

762

763

764

765

766

767

768

769

770

771

772

773

774 ANATOMY OF A LOCAL-SCALE DROUGHT: APPLICATION OF ASSIMILATED REMOTE SENSING PRODUCTS,
775 CROP MODEL, AND STATISTICAL METHODS TO AN AGRICULTURAL DROUGHT STUDY

776

777

778 **Figures**

779

780

781

782

783

784

785

786

787

788

789

790

791

792

793

794

795

796

797

798

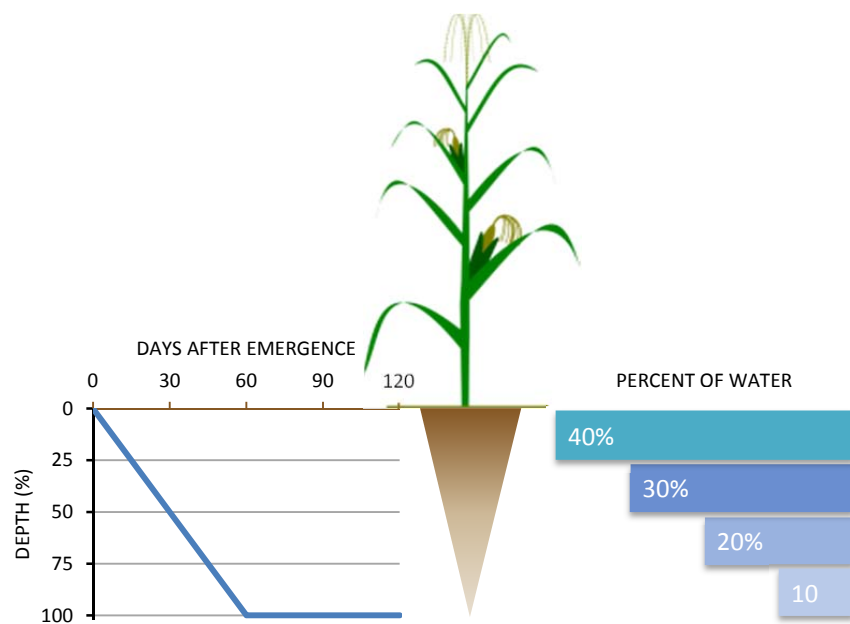
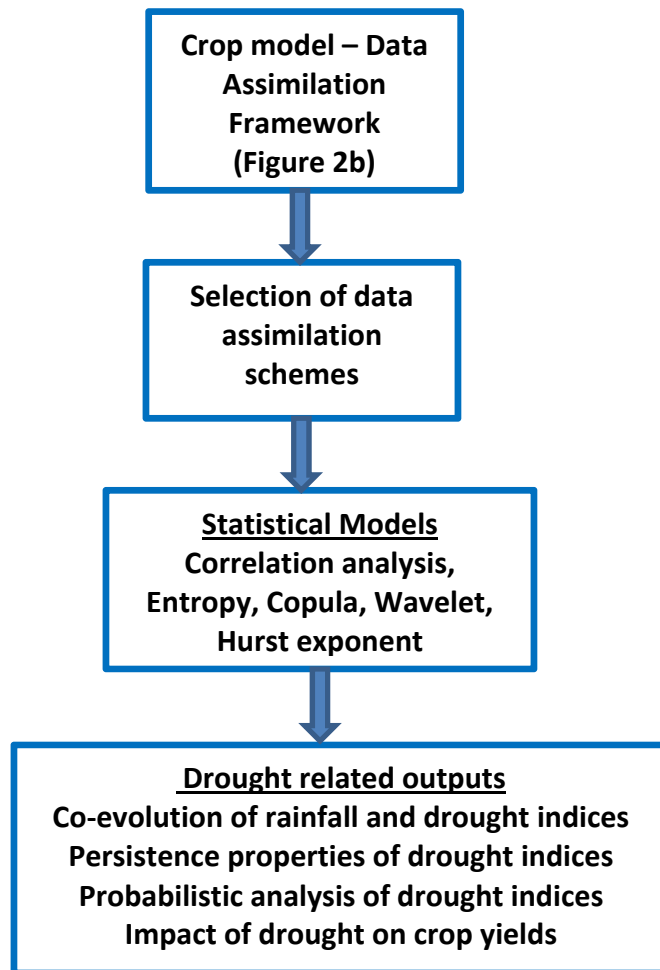


Figure 1. Variation of soil water extraction by Corn with respect to depth and **plant root development patterns** (Kranz et al., 2008).

799
800
801
802
803
804
805
806
807
808
809
810
811
812
813
814
815
816
817
818
819
820
821
822
823



824

825

Figure 2a. Framework for local scale drought study using combination of models.

826

827

828

829

830

831

832

833

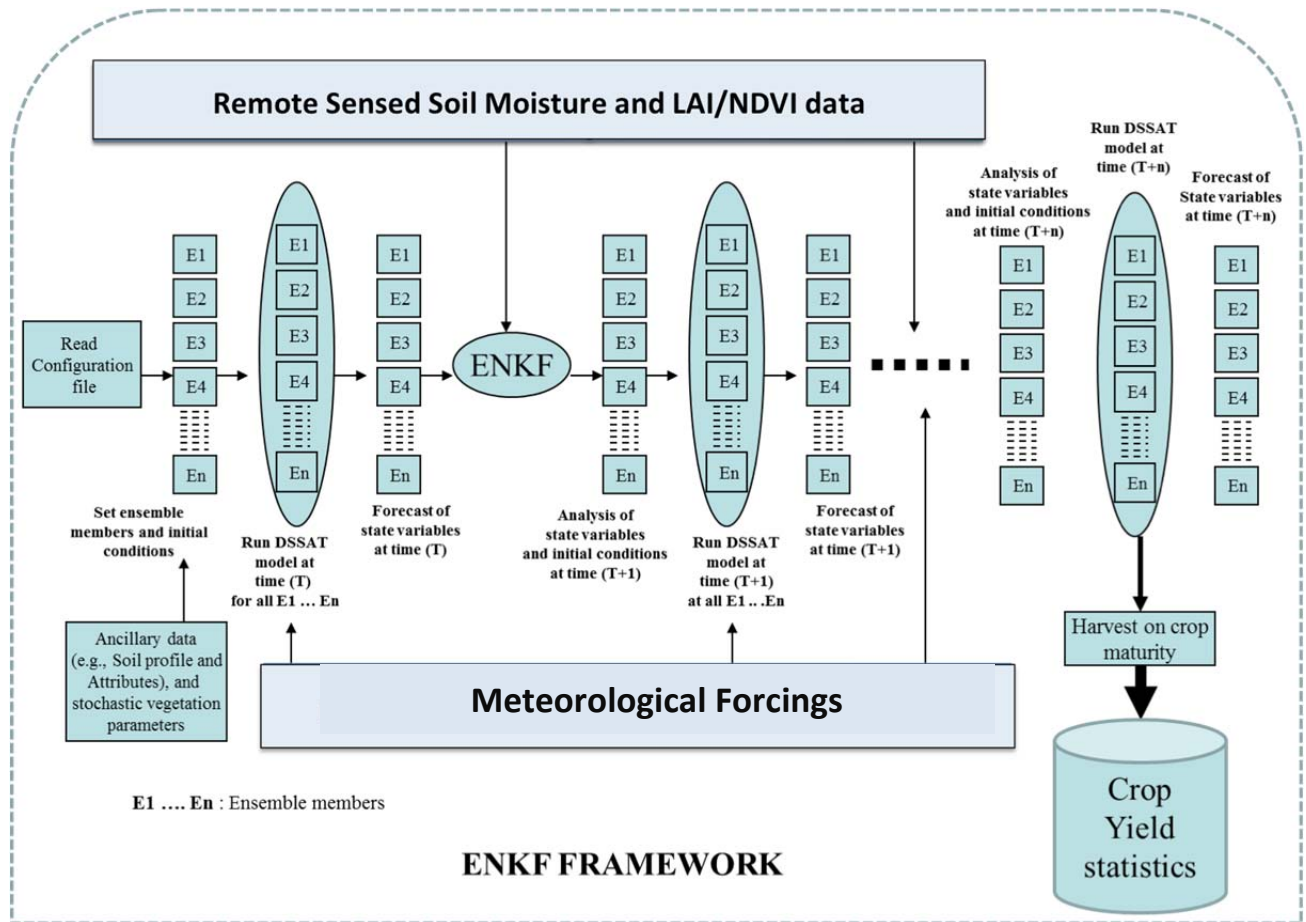
834

835

836

837

838



839

840

Figure 2b. Crop model-data assimilation framework (Ines et al. 2013).

841

842

843

844

845

846

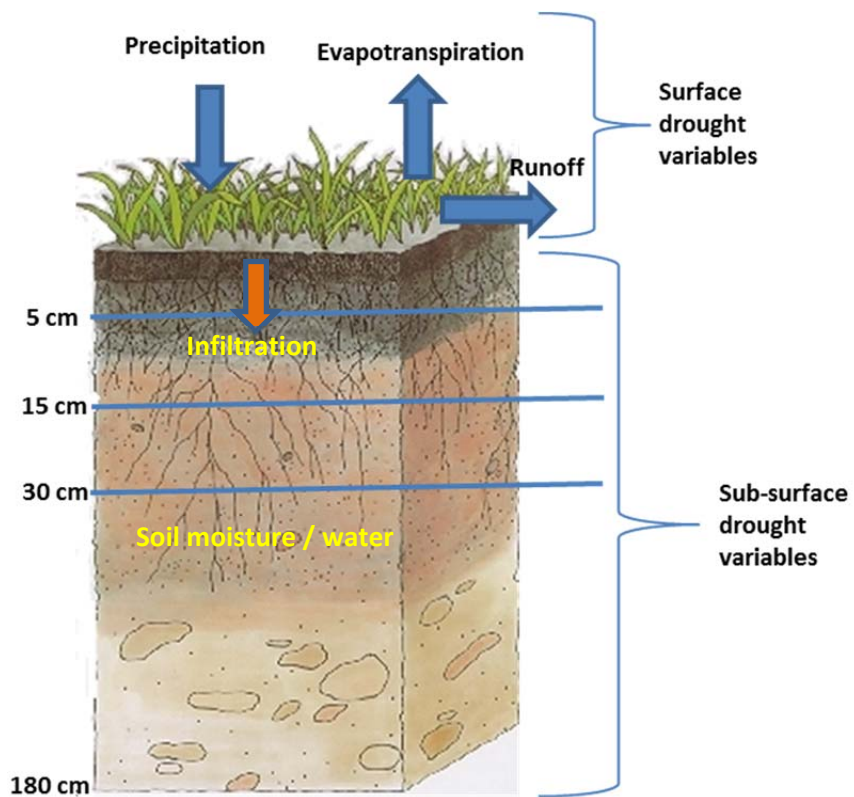
847

848

849

850

851



852

853

Figure 3. Distinction between surface and subsurface drought variables

854

855

856

857

858

859

860

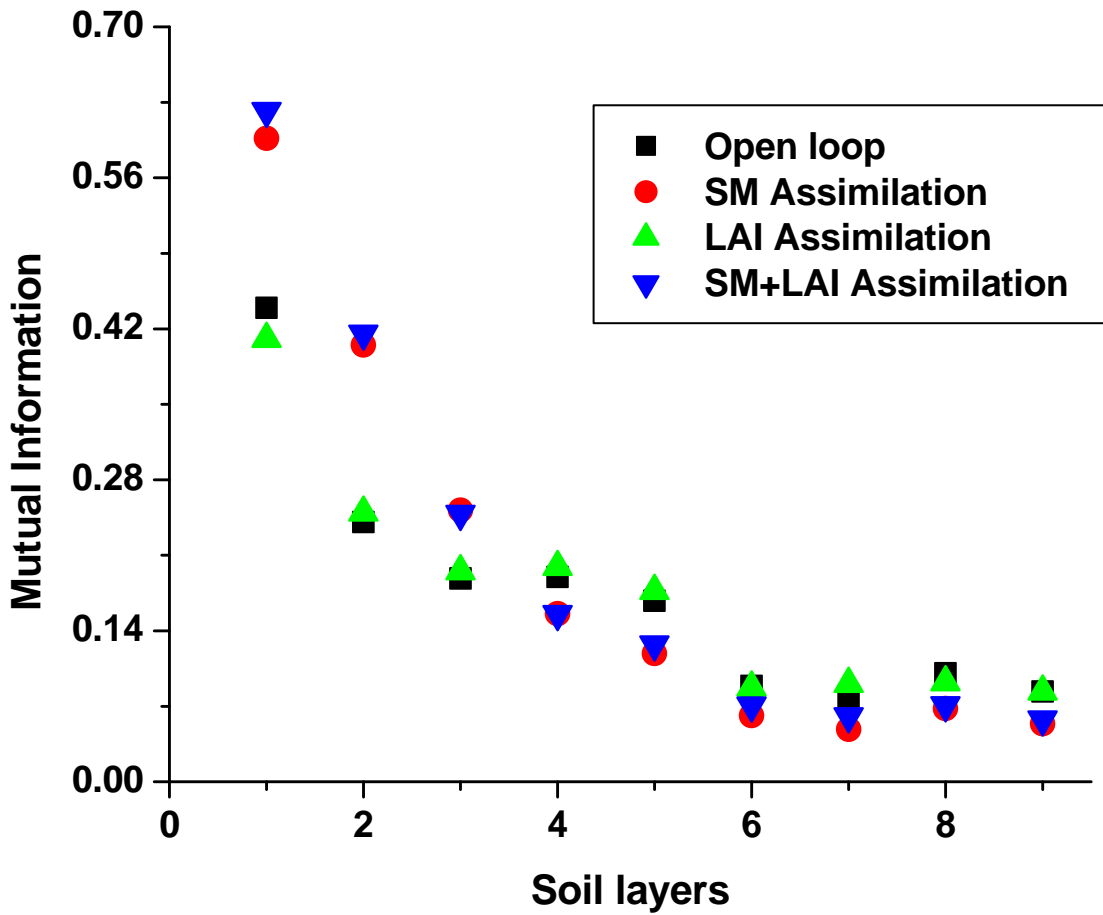
861

862

863

864

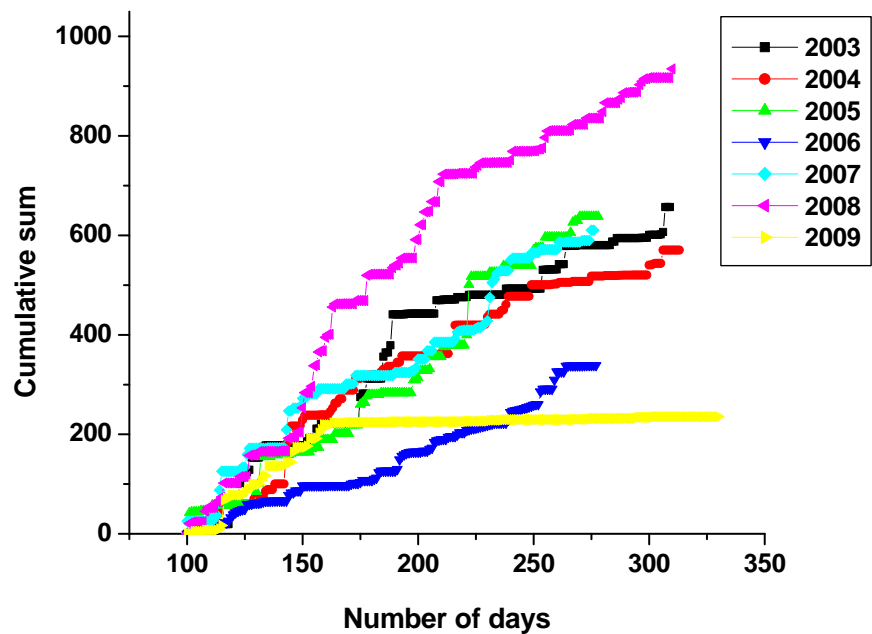
865
866
867
868



869
870
871
872
873
874
875
876
877

Figure 4. Mutual information between weekly rainfall and soil moisture at different layers based on different assimilation schemes.

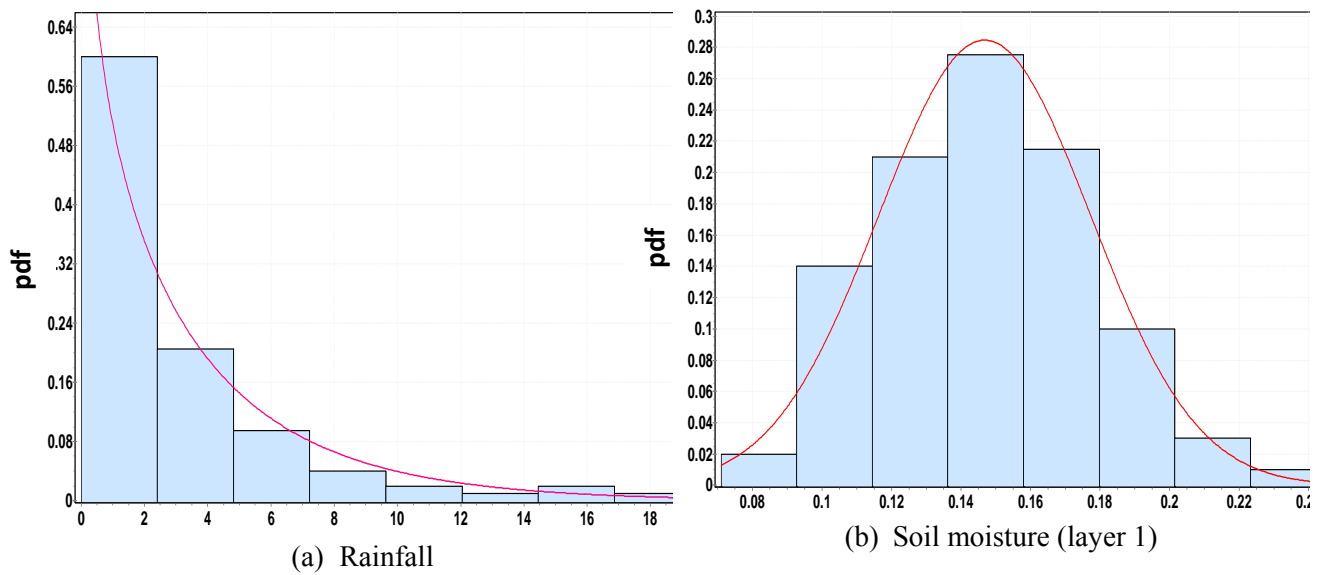
878
879
880
881
882
883



884
885
886
887
888
889
890
891
892
893
894

Figure 5. Cumulative precipitation pattern during crop periods for different years.

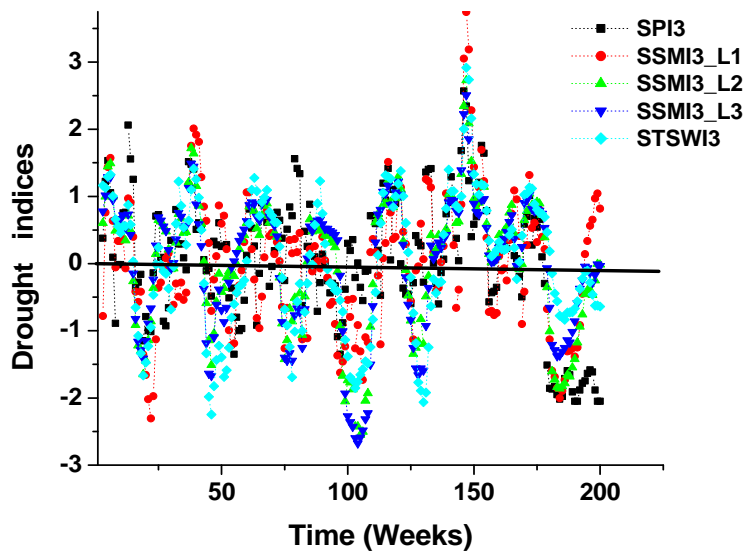
895
896
897
898
899
900
901
902
903
904
905



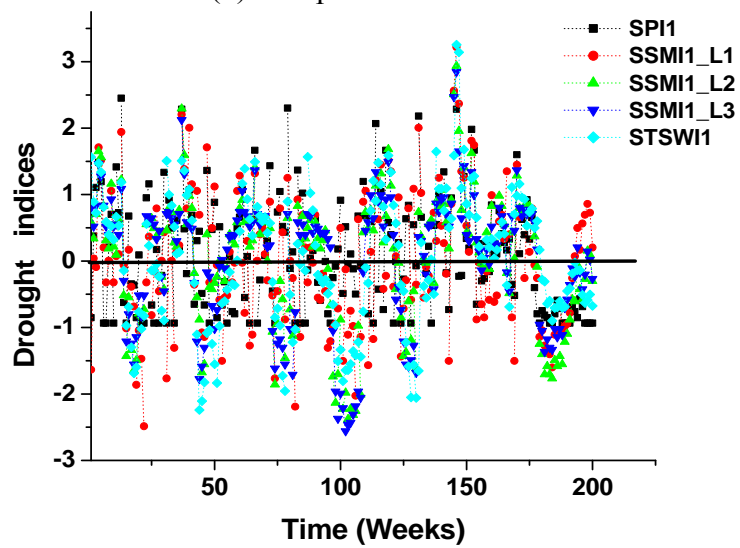
906
907
908
909
910
911

Figure 6. Probability density function of weekly rainfall and soil moisture (layer 1)

912
913
914
915
916
917
918
919



(b) Temporal scale 3 weeks



(a) Temporal scale 1 week

920 **Figure 7.** Time series plot of different drought indices during crop period for 2003-2009. [Note
921 that x-axis represents duration of crop periods for different years: 2003 (1-30 weeks), 2004 (31-
922 61 weeks), 2005 (62-87 weeks), 2006 (88-112 weeks), 2007 (113-137 weeks), 2008 (138-167
923 weeks), and 2009 (168-200 weeks)].

924

925

926

927

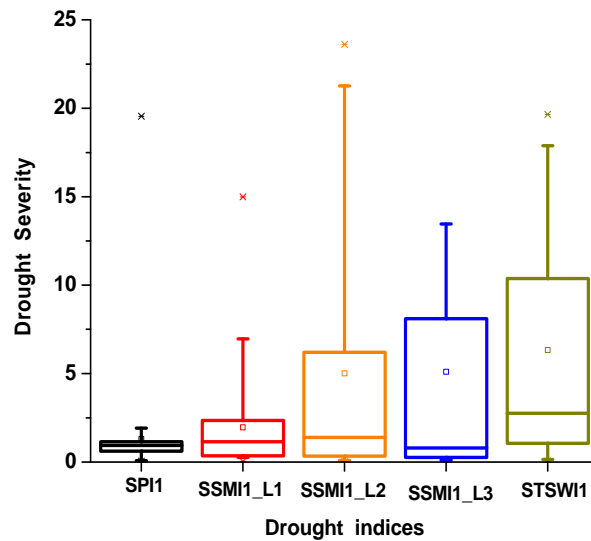
928

929

930

931

932



933 **Figure 8.** Box plot of the drought severity of drought indices at 1 week temporal scale.

934

935

936

937

938

939

940

941

942

943

944

945

946

947

948

949

950

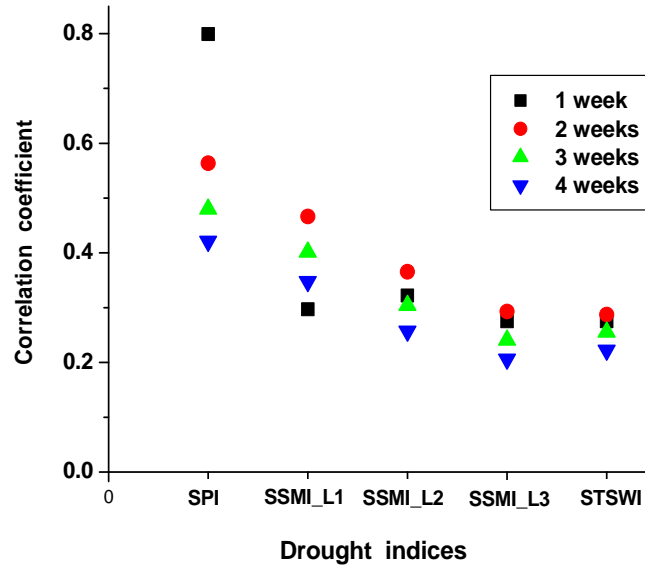
951

952

953

954

955



956

Figure 9. Cross correlation plot between weekly rainfall and drought indices of different temporal scales.

957

958

959

960

961

962

963

964

965

966

967

968

969

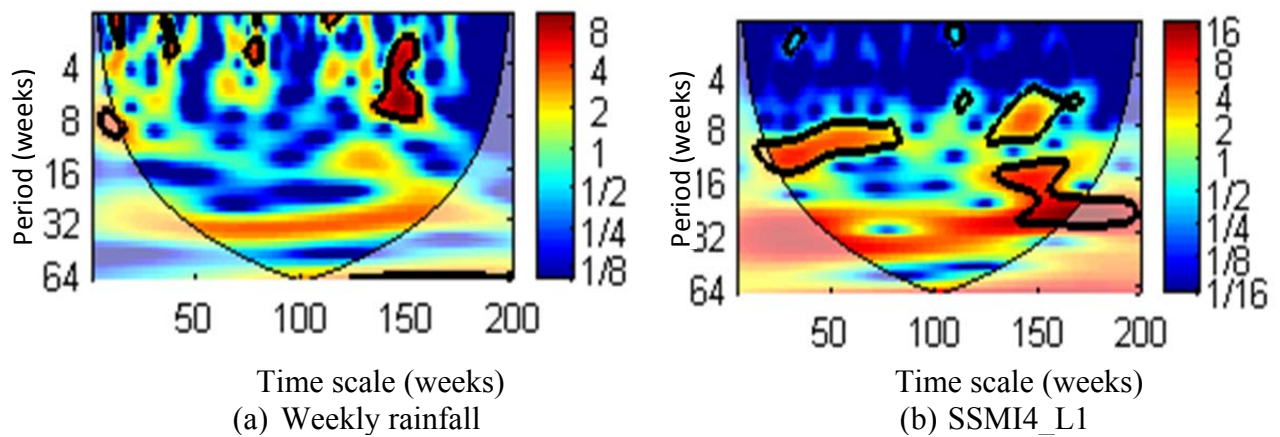
970

971

972

973

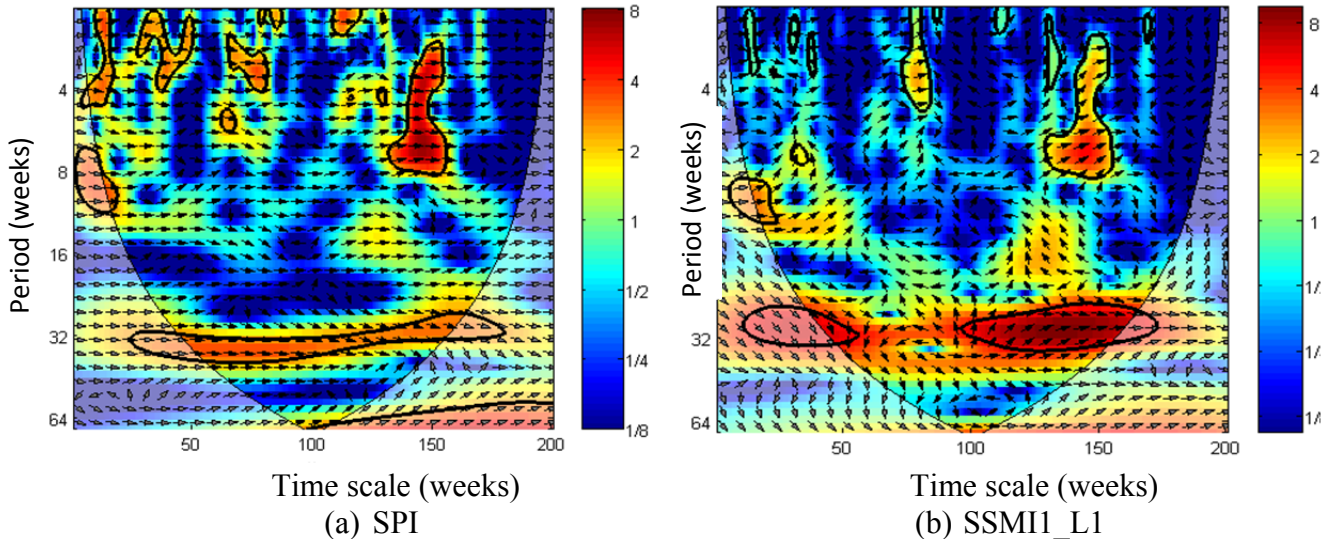
974
975
976
977
978
979
980



981 **Figure 10.** Wavelet analysis of weekly rainfall and standardized soil moisture index for layer 1
982 at temporal scale of 4 week (SSMI4_L1). [Note that x-axis represents duration of crop periods
983 for different years: 2003 (1-30 weeks), 2004 (31-61 weeks), 2005 (62-87 weeks), 2006 (88-112
984 weeks), 2007 (113-137 weeks), 2008 (138-167 weeks), and 2009 (168-200 weeks)].

985
986
987
988
989
990
991
992
993

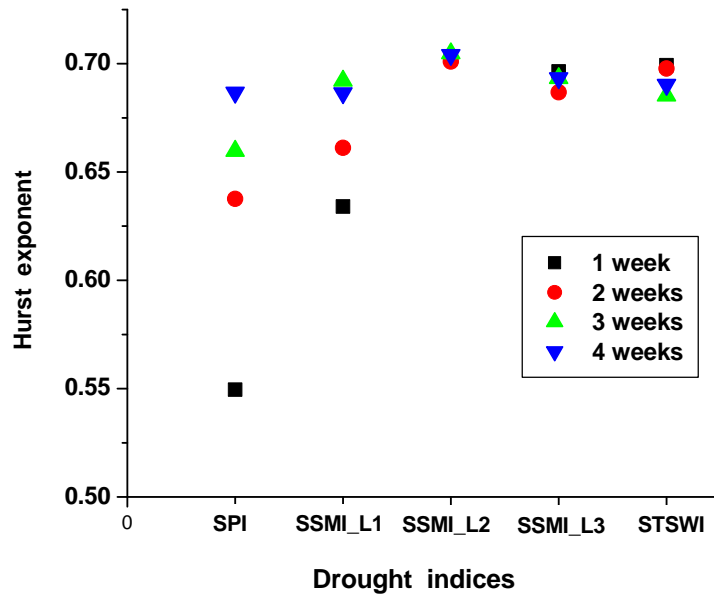
994
995
996
997
998
999
1000
1001



1002 **Figure 11.** Cross wavelet analysis between: (a) weekly rainfall and SPI1 standardized soil
1003 moisture index for layer 1 at temporal scale of 4 weeks (SSMI4_L1). [Note that x-axis represents
1004 duration of crop periods for different years: 2003 (1-30 weeks), 2004 (31-61 weeks), 2005 (62-
1005 87 weeks), 2006 (88-112 weeks), 2007 (113-137 weeks), 2008 (138-167 weeks), and 2009 (168-
1006 200 weeks)].

1007
1008
1009
1010
1011
1012

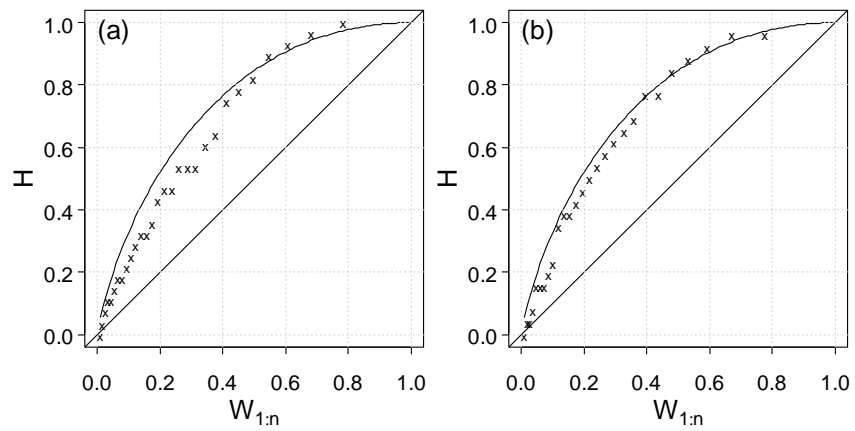
1013
1014
1015
1016
1017
1018
1019
1020
1021
1022
1023
1024
1025



1026
1027
1028
1029

Figure 12. The Hurst exponent (H) of drought indices at different temporal scale.

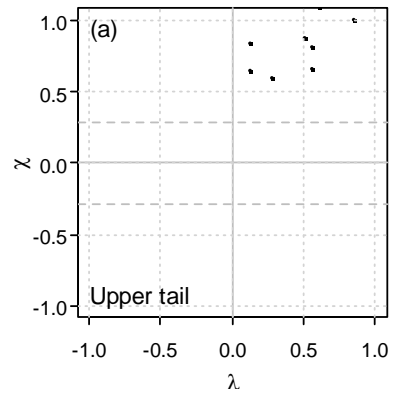
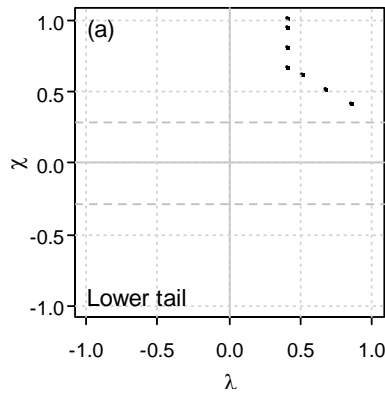
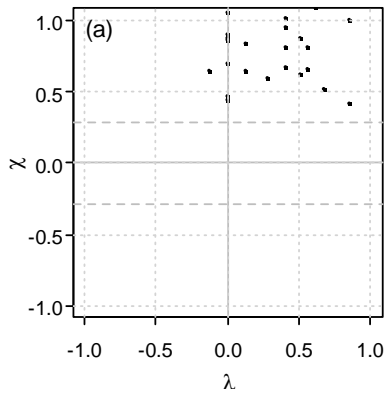
1030
1031
1032
1033
1034
1035
1036
1037
1038
1039
1040
1041
1042
1043
1044
1045

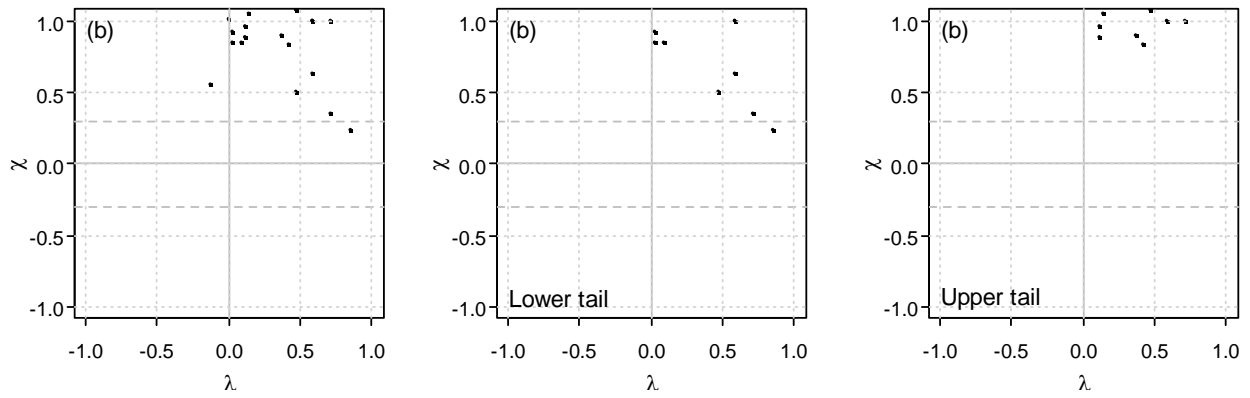


1046
1047
1048
1049

Figure 13. Kendall's plots exploring the dependence structure between drought duration and severity for (a) SPI2, (b) SSMI2_L1, (c) SMI2_L2

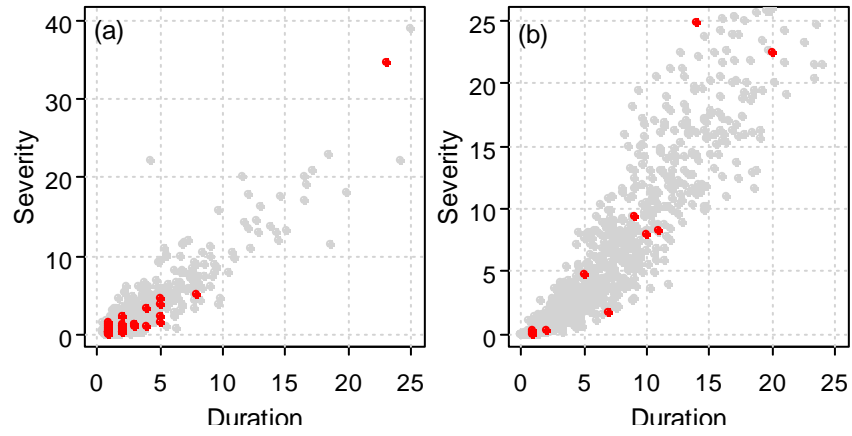
1050
1051
1052
1053
1054
1055
1056
1057
1058
1059
1060
1061
1062
1063
1064
1065
1066
1067
1068





1069 **Figure 14.** Chi-plots exploring the dependence structure between drought duration and severity
 1070 for (a) SPI2, (b) SSMI2_L1. The first column shows the complete set of data and the second and
 1071 third column shows the lower and upper tail respectively.

1072
 1073
 1074
 1075
 1076
 1077
 1078
 1079
 1080
 1081
 1082
 1083
 1084
 1085
 1086



1087

1088

1089

Figure 15. Comparison of observed (red dots) and simulated values (gray dots) from the most suitable copula for (a) SPI2, and (b) SSMI2_L2.

1090

1091

1092

1093

1094

1095

1096

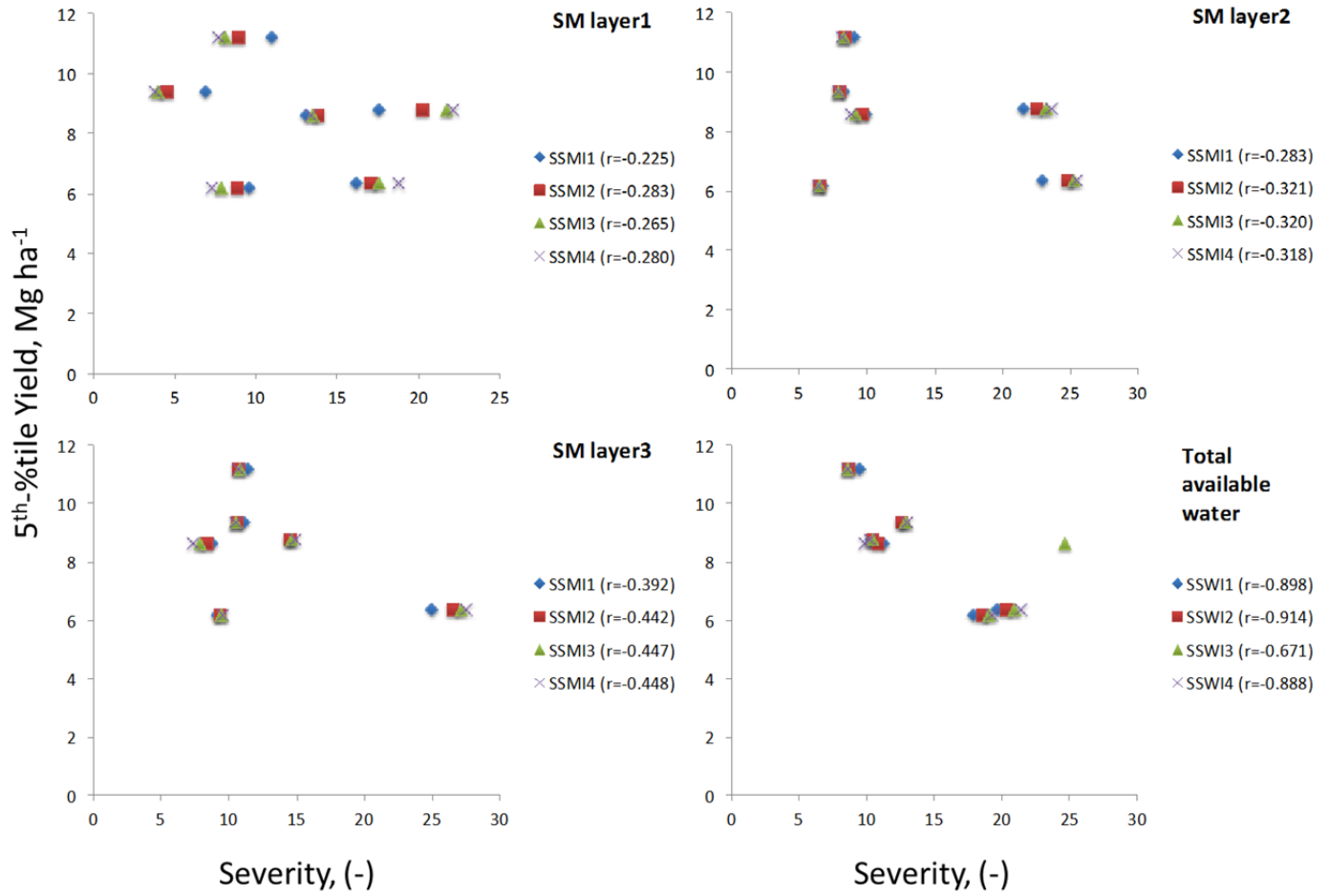
1097

1098

1099

1100

1101



1102

1103 **Figure 16.** Maize yields (5th %-tile) and drought severity index relationship. The correlation coefficient
 1104 values are provided in parenthesis.
 1105

1106

1107

1108

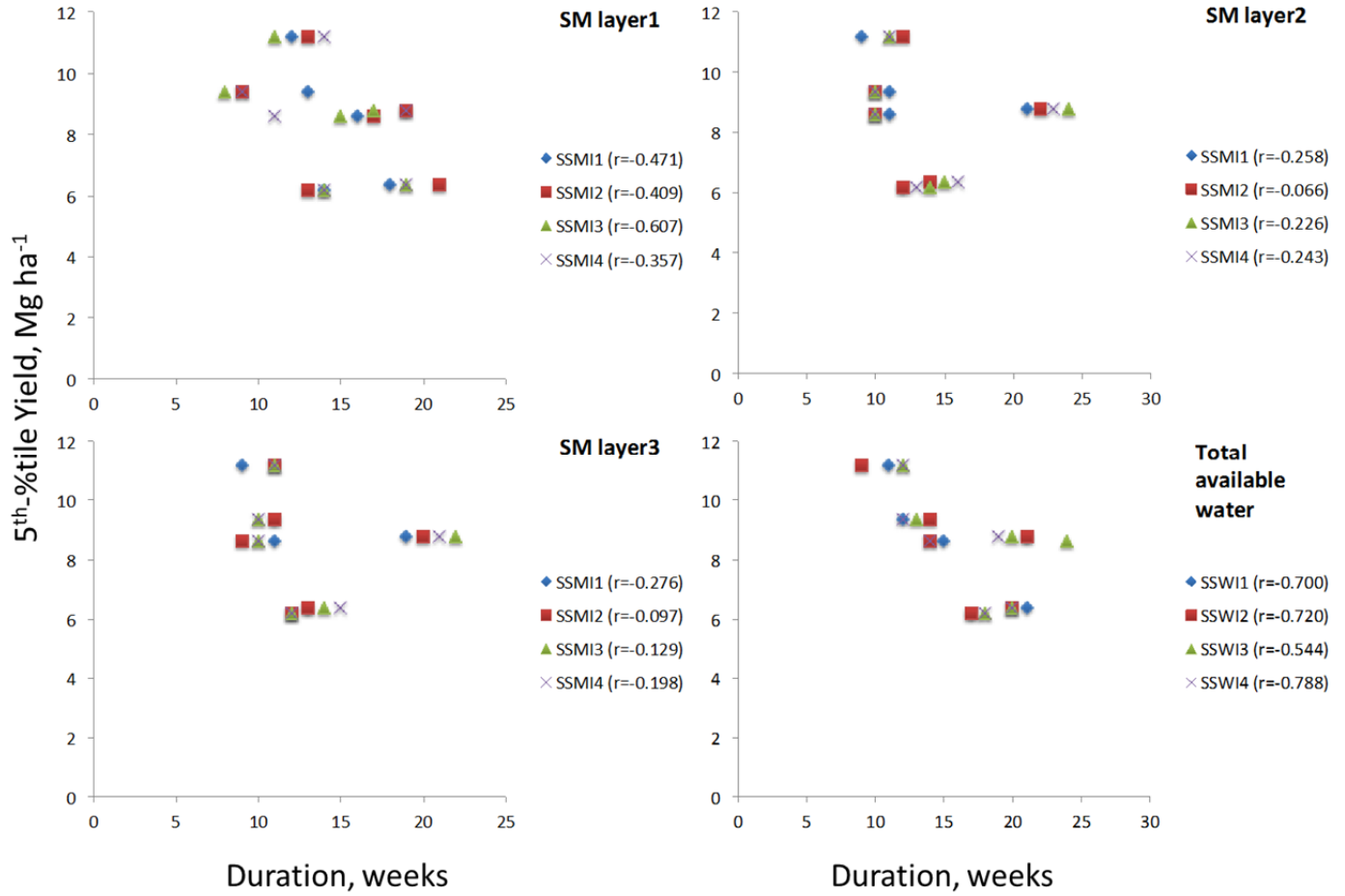
1109

1110

1111

1112

1113



1114

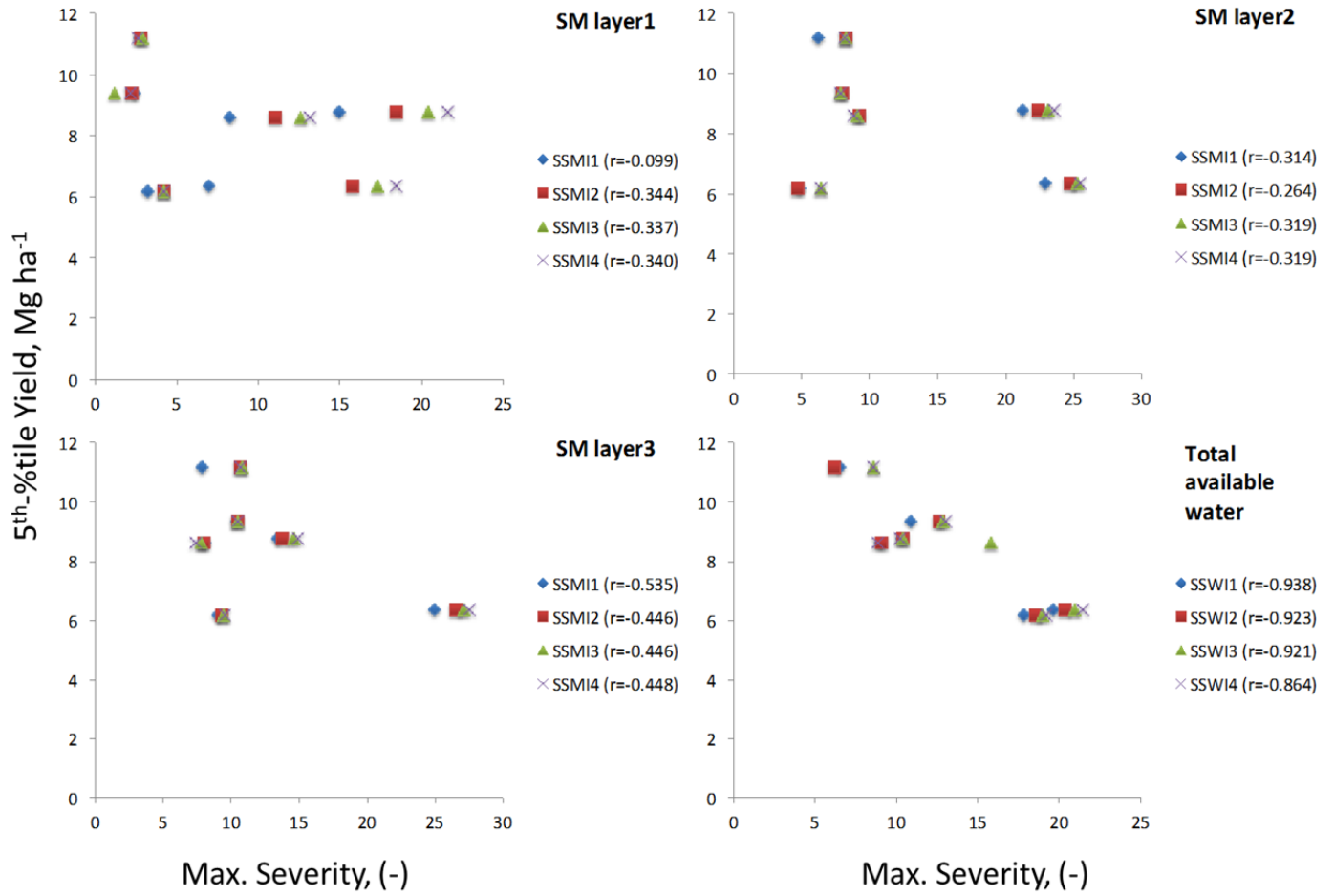
1115 **Figure 17.** Maize yields (5th %-tile) and drought duration index relationship.

1116

1117

1118

1119



1120

1121

Figure 18. Maize yields (5th %-tile) and drought maximum severity index relationship.

1122

1123

1124

1125

1126

1127

1128

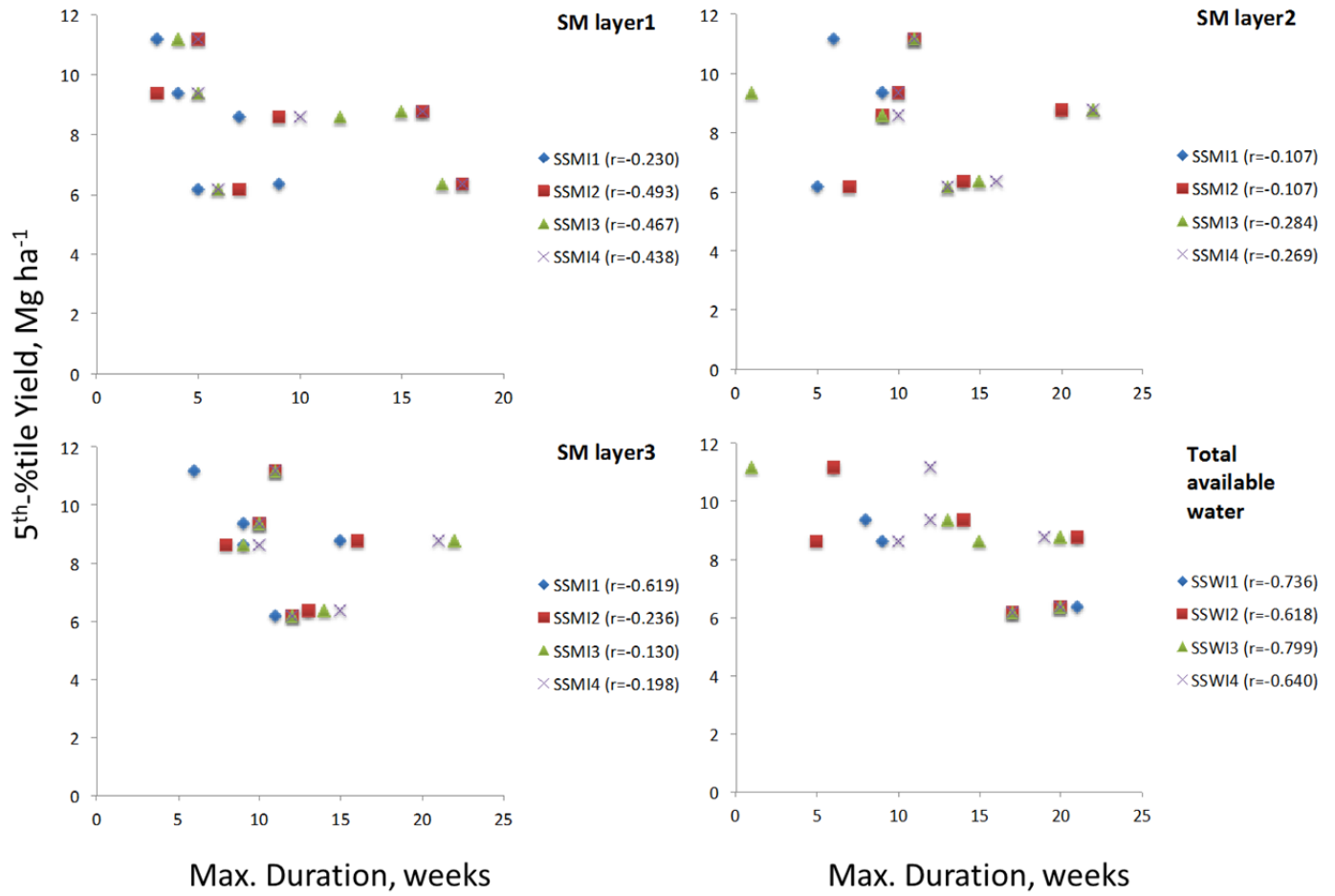
1129

1130

1131

1132

1133



1134

1135 **Figure 19.** Maize yields (5th %-tile) and drought maximum duration index relationship.

1136

1137

1138

1139

1140

1141

List of Tables

1142

1143

1144 **Table 1.** Performance (average) of the crop model-data assimilation (DA) system for simulating
 1145 maize yields, Story County, Iowa (after Ines et al., 2013).

Experiment	R	MBE, Mg ha ⁻¹	RMSE, Mg ha ⁻¹
Openloop:	0.47	-3.7	4.7
DA with LAI:	0.51	-3.2	4.2
DA with SM:	0.50	-1.9	3.6
DA with SM + LAI:	0.65	-2.0	2.9
Composite best (SM + LAI, LAI):	0.80	-1.2	1.4

1146 R – Pearson’s correlation

1147 MBE – Mean Bias Error

1148 RMSE – Root Mean Squared Error

1149

1150

1151

1152 **Table 2.** Most appropriate copula for SPI, SSMI and SSWI

<i>Variable</i>	<i>1 week</i>	<i>2 weeks</i>	<i>3 weeks</i>	<i>4 weeks</i>
SPI	Joe	Joe	Gumbel	Gumbel
SSMI_L1	Joe	Joe	Gaussian	Gaussian
SSMI_L2	Frank	Gaussian	Gaussian	Clayton
SSMI_L3	Frank	Frank	Clayton	Gaussian
SSWI	Gaussian	Clayton	Student t	Joe

1153

1154

1155

1156